UNIVERSITÄT KOBLENZ · LANDAU
Fachbereich 4: Informatik

TECHNISCHE UNIVERSITÄT WIEN
VIENNA UNIVERSITY OF TECHNOLOGY

Volume Hatching for Illustrative Visualization

Diplomarbeit

zur Erlangung des Grades eines Diplom-Informatikers
im Studiengang Computervisualistik

vorgelegt von
Moritz Gerl

Erstgutachter:	Prof. Dr.-Ing. Stefan Müller (Institut für Computervisualistik, AG Computergraphik)
Zweitgutachter:	Ao.Univ.Prof. Dr. Eduard Gröller
Betreuender Assistent:	Dipl.-Ing. Stefan Bruckner (Technische Universität Wien, Institut für Computergraphik und Algorithmen, AG Visualisierung)

Koblenz, im November 2006

Erklärung

Ich versichere, dass ich die vorliegende Arbeit selbständig verfasst und keine anderen als die angegebenen Quellen und Hilfsmittel benutzt habe.

	Ja	Nein
Mit der Einstellung der Arbeit in die Bibliothek bin ich einverstanden.	☐	☐
Der Veröffentlichung dieser Arbeit im Internet stimme ich zu.	☐	☐

.....

(Ort, Datum) (Unterschrift)

Contents

1 Introduction

The evolution of drawing reaches back to the origin of human cultural history. Over 20.000 years ago prehistoric men started to picture their environment in petroglyphs. From these caveman paintings to mythological depictions of the ancient Egyptians, from medieval illuminated manuscripts to Leonardo Da Vinci's anatomical studies in the Renaissance, drawings served the purpose of transforming information into a visually perceptible form. Maybe it is this historical tradition that gives drawings the character of being perceived as beautiful by a widespread public. Maybe it is the abstract nature of drawings that lets them be an art form commonly chosen for illustration. Often the first type of imagery we deal with in our lifetime are hand-drawn images in children's books. So we literally grow up with drawings as a familiar medium for depiction. This could also be a cause for the high acceptance drawings usually meet.

Drawings are commonly used in a scientific and educational context to convey complex information in a comprehensible and effective manner. Illustration demands abstraction for focusing attention on important features by avoiding irrelevant detail. Abstraction is a characteristic inherent in drawing, as a drawing always abstracts real world. Therefore drawings serve the purpose of illustration very well. In addition to that, the expressiveness and attraction of drawings bestow them the property of communicating information in a way mostly felt as enjoyable.

Specific applications of volume visualization require exactly these visual properties. Therefore increasing effort has been spent on developing and applying illustrative or non-photorealistic rendering methods for volume visualization in recent years. This is the field of study this thesis is devoted to. The described capabilities of drawing make it the art form we chose to mimic for the non-photorealistic volume rendering approach developed in this thesis. A common shading technique in drawings is hatching. Hatching is also standard practice in schematic hand-drawn illustrations as known from textbooks. We implemented a system capable of generating hatching drawings from volume datasets. The basic idea was to exploit illustrative and aesthetic excellence of hatching drawings for the creation of expressive representations of volumetric data.

The drawing in Figure 1 gives an example of an illustration where hatching has been used for shading. This figure shall demonstrate that hatching is a technique capable of conveying spatial properties of the depicted object in an abstract and expressive way. It is an artwork of Vesalius' *De humani corporis fabrica*, a textbook of human anatomy from the Renaissance.

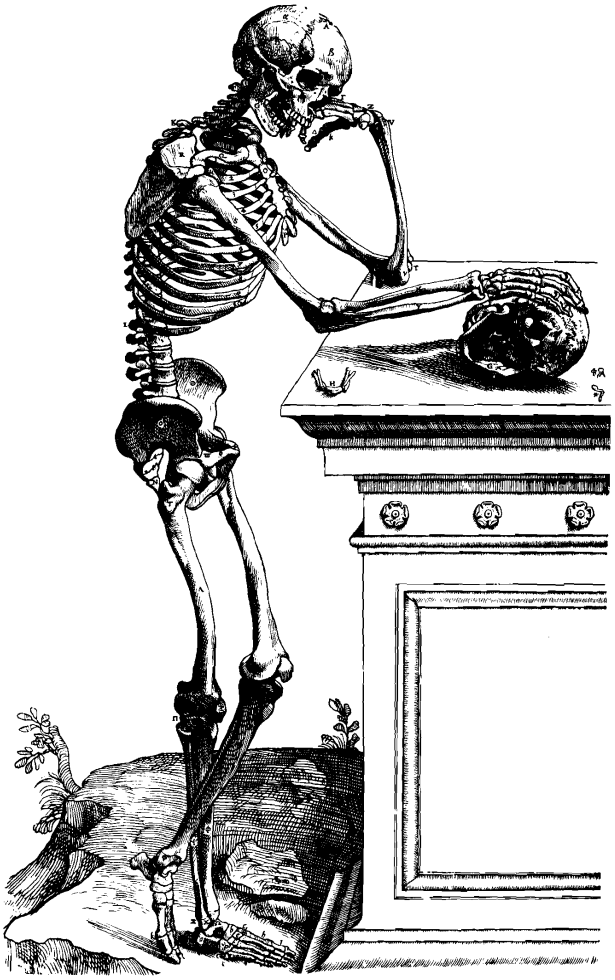

Figure 1: Hatching drawing by Vesalius.

We propose some possible fields of application to further explain the motivation to engage in generating hatching drawings from three-dimensional data. The majority of these data are generated in medical scanning devices, and medicine offers numerous possibilities for employing volume hatching. One possible medical application would be to illustrate upcoming surgeries to patients. Explaining a surgery with the help of a volume hatching rendering is perhaps more comprehensible for a layman than with tomography slices. It also could be more readily accepted by patients as a realistic rendering, due to the visually pleasing nature of hand drawings and the distaste of some people on viewing inner body parts realistically.
Another potential field of application for volume hatching is the automated generation of educational illustrations. Figures in scientific textbooks, for instance in medicine or botany, which shall convey important structural features by a schematic representation of objects, are often drawn by hand. The preferred drawing medium here is pen-and-ink, and a reduced drawing technique is used where shading is realized with a sparse and even hatching. Volume hatching can be employed for creating images resembling such illustrations from volumetric data. On the one hand, this offers the possibility for automated generation of still images for text- or schoolbooks. On the other hand, interactive illustrations could be applied in teaching, since they provide exploration and examining possibilities while depicting the objects in a familiar illustrative style.
This thesis is organized as follows. First, we give an overview about research done in fields related to this thesis in Chapter 2. In Chapter 3 we present the algorithms we developed for rendering hatching drawings from volume data. This includes the creation of contour drawings, curvature estimation and generation of hatching strokes. We continue with shortly outlining the concept of implementing these algorithms in Chapter 4. In Chapter 5 we present and discuss result images, revealing advantages and limitations of our approach. We summarize the content of this thesis in Chapter 6. Finally, we draw a conclusion on the results of this thesis and propose ideas for further enhancing our work in Chapter 7.

2 Related Work

This chapter will outline the current state of research in computer graphics disciplines related to this thesis. We begin with a brief overview of existing volume rendering approaches. Thereafter relevant features of the field of illustrative or non-photorealistic rendering (NPR) will be presented. Finally, applications of non-photorealistic rendering techniques to volume visualization will be summarized.

2.1 Volume Rendering

The subject matter of volume visualization are volumetric datasets, commonly given as regular three-dimensional grids of sample values denoted as voxels. The majority of volumetric datasets are produced in medical imaging processes and therefore represent density values of organic tissues. For the task of transforming these datasets into a visually perceptible form, several approaches have been proposed.
One way of rendering a volumetric dataset is to create proxy geometry which is pictured with traditional computer graphics methods. The other way, which will be discussed here, is rendering the volume directly abdicating the need for computing an intermediate geometric representation. These approaches can be classified by the order the data is being processed into image-order, object-order and hybrid-order methods. Newer techniques utilize programmable graphics hardware for volume rendering. Direct volume rendering concepts involve an illumination model and a so-called transfer function, which maps scalar values of the dataset to color and opacity values. A surface within a volume satisfying the constraint that all voxels contain the same intensity value is denoted as iso-surface.

2.1.1 Image-Order Volume Rendering

In image-order volume rendering, the pixels on the image plane are being traversed computing the contribution of the corresponding voxels to each pixel. A common image-order algorithm is raycasting [28]. This algorithm casts viewing rays into the volume, starting at image plane pixels.
In fixed intervals along the ray, the volumetric signal is reconstructed from

the samples and optical properties at the resample locations are determined. The color information gained along the ray is accumulated and results in the pixel color value.
Several publications [30, 29, 39, 24] deal with increasing the performance of the basic raycasting algorithm. The image quality attained with raycasting is very high, often regarded as the best among the volume rendering approaches, respectively competing with the image quality of splatting which we will discuss next.

2.1.2 Object-Order Volume Rendering

Object-order volume rendering techniques traverse the dataset and calculate each voxel's contribution to the image. Splatting [56] is a well-known object-order algorithm which processes the voxels, evaluates the optical model and projects the color contributions onto the image plane.
Further research enhancing this approach aims at improving the image quality [35] and performance [36] of splatting.

2.1.3 Hybrid-Order Volume Rendering

The shear-warp algorithm [26] was proposed intending to combine advantages of image-order and object-order methods. The shear-warp algorithm decomposes the viewing transformation into a shear and a warp transformation. Shearing the volume slices yields sampling rays parallel to the principal viewing direction. This allows for traversing volume and image simultaneously. An intermediate projection is calculated and subsequently warped onto the image plane.
The shear-warp algorithm is a very efficient software volume rendering algorithm, but suffers from a low image quality. This is due to the fact that only bilinear interpolation is available during reconstruction.
Some work [48] has been done to enhance the low image quality of the shear-warp algorithm.

2.1.4 GPU-Based Volume Rendering

With the increase of the computing power of graphics hardware, approaches were developed which apply the programmability of the Graphics Processing Unit (GPU) to volume visualization.
One way to use the GPU for volume rendering is exploiting $2D$ texture mapping functionality [42]. A common technique stores three stacks of $2D$ textures, one for each major viewing axis. The stack corresponding the most to the viewing direction is chosen and its textures are mapped on object-aligned quads which are rendered with alpha blending.
Other methods utilize the $3D$ texture mapping capability of GPUs [4, 12, 55, 34]. Thereby, the whole dataset is used as a $3D$ texture. This volume texture is mapped onto view-aligned quads which are rendered using alpha blending. One problem of $3D$ texture mapping is the limitation of available video memory.
As the functionality of programming the GPU has expanded in the last years, it is now possible to implement traditional volume rendering algorithms such as raycasting to be performed on the GPU [46, 15].

2.2 Non-Photorealistic Rendering

In contrast to traditional computer graphics disciplines, which are concerned with generating realistic images, the area of non-photorealistic rendering (NPR) deals with creating imagery in artistic or expressive styles.
Research in the area of NPR has enabled mimicking a wide variety of styles used in visual arts with computer graphics methods. Painterly rendering for instance deals with the simulation of watercolor [6] or oil [16] paintings. Other NPR techniques employ alternative shading models such as cartoon and metal shading [13] to implement diverse rendering styles. We will here focus on related work concerned with hand drawn imagery, namely line drawing, pencil and pen-and-ink drawing. We start by examining research on contour-depicting line drawings, then have a look at pen-and-ink rendering and finally survey techniques which produce hatching and pencil drawings from polygonal data.

2.2.1 Line Drawing

Line drawings are conventionally used for illustrations, and the line is a commonly used primitive in computer graphics. Numerous researchers have developed strategies for creating line drawings with the computer.
Interrante et al. [19] propose ridge and valley lines for rendering transparent skin surfaces. In order to enable a simultaneous display of multiple layers of data, lines depicting important shape features are detected and rendered appropriately to augment the spatial perception of the rendering. The quality of line drawings has been further enhanced by methods such as varying the line width, as proposed by Gooch et al. [14].
To further improve conventional computer generated line drawings, DeCarlo et al. [7] introduced suggestive contours. They compute additional contour lines for conveying the shape of the depicted object. These additional lines are placed in areas with high curvature alteration and reveal structures which are not visible in images generated with simple contour drawing techniques. Figure 2 shows the effect of conveying shape with suggestive contours.

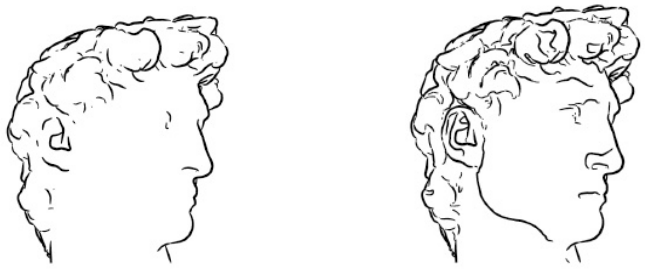

(a) (b)

Figure 2: Additional feature lines. Image (a) without, (b) with suggestive contours. Images courtesy of DeCarlo et al. [7].

McGuire and Hughes [33] present an edge detection and drawing algorithm for hardware implementation. They use a data structure referred to as edge mesh to transfer information about edges to the GPU in the form of vertex attributes. They perform a per-edge contour recognition and use stroke textures to achieve a hand-drawn appearance.

Markosian et al. [32] are concerned with efficient silhouette rendering of $3D$ models with different drawing styles. They use a modification of a common hidden line removal algorithm for an efficient visibility determination. They manage to identify silhouette edges and render them maintaining inter-frame coherence at interactive rates.

2.2.2 Pen-And-Ink Rendering

Pen-and-ink drawings are an expressive medium and a favored technique among illustrators. Its clearness and directness originate from the circumstance that all visual properties such as shape, shade and texture of the object to be drawn have to be suggested just by the arrangement and size of individual strokes. Pen-and-ink offers just one color and tone.
Winkenbach and Salesin [57] propose a method to render computer generated pen-and-ink illustrations of $3D$ models. They introduce the concept of stroke textures for mimicking different drawing styles and materials. A stroke texture contains multiple strokes arranged in regular patterns which represent various materials. It has to convey both tone and texture, whereby a darker tone is achieved through a higher density of strokes. They prioritize the strokes in order to render them sequentially until the desired tone is obtained. They emphasize the need for a tight linkage of texture and tone, which are usually separated in the rendering pipeline, and the importance of a combination of $2D$ and $3D$ information. Winkenbach and Salesin depict boundary outlines via drawing strokes of a boundary edge with a dedicated texture. The interior outlines are used for accentuating strokes or suggesting shadow directions. Outline strokes are minimized by drawing a contour stroke only if the tones of its adjacent faces differ sufficiently. Outline strokes are also used to assist the spatial impression by varying the line thickness according to local illumination properties and the viewing direction. They improve the quality of their results with a semi-automated method for placing indication in the drawings. The user interactively attaches detail segments to areas which shall be drawn more detailed. Figure 3 displays an example image for their approach.

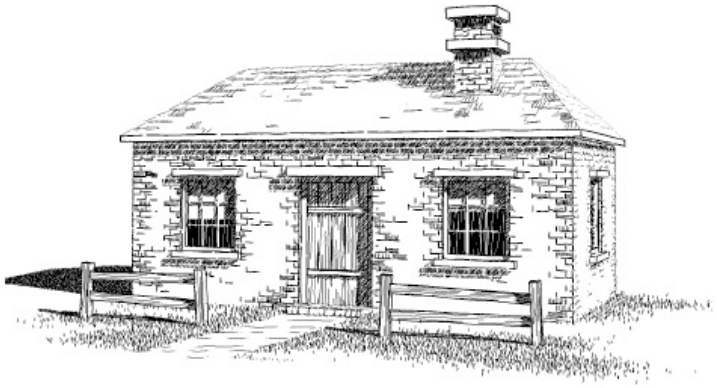

Figure 3: Pen-and-ink rendering of a polygonal mesh. Image courtesy of Winkenbach and Salesin [57].

Salisbury et al. [44] introduce an interactive system for producing pen-and-ink renderings. The user paints with a stroke texture as discussed above. It is possible to paint a multitude of strokes with one mouse click. Dragging the mouse allows to modify the tone in an area of interest. The user can pick a desired texture out of a stroke texture library. The strokes within a texture are prioritized. During drawing adequate strokes are selected until the required tone is achieved. Additionally, individual strokes can be drawn or modified by the user and also collections of strokes can be modified for simultaneously altering multiple strokes. They provide the user with the possibility to underlay the drawing area with a reference image to augment the creation of drawings with the interactive toning system. Figure 4 shows result images.

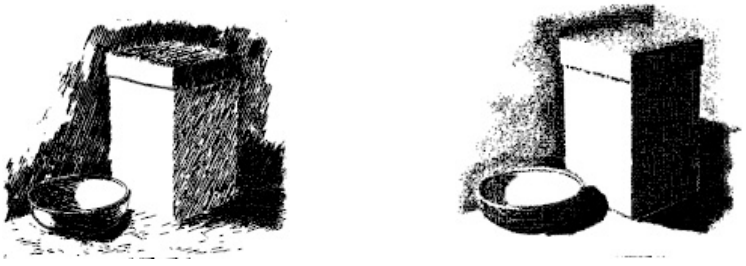

Figure 4: Interactive pen-and-ink rendering. Images courtesy of Salisbury et al. [44].

2.2.3 Pencil Drawing and Hatching

Praun et al. [41] proposed an interesting approach for creating hatchings from $3D$ models in real time. Hatching strokes over arbitrary surfaces are drawn to convey material, tone and form of the model. They introduce the concept of Tonal Art Maps, compilations of mipmapped textures corresponding to various tones and resolutions. A texture of a Tonal Art Map contains multiple strokes. The density of strokes corresponds to the tone the texture represents. A Tonal Art Map is computed in a preprocessing step and used for texturing a $3D$ model with appropriate stroke textures. One constraint during the creation of the strokes of the Tonal Art Map textures is a nesting property. All strokes of textures with a lighter tone appear in those of darker tones, so a tone variation can be depicted coherently and smoothly. In order to obtain a consistent stroke size and density in all resolutions, the hatching strokes are scaled according to the resolution and the mipmap levels are used for different primitive sizes. To gain an evenly spacing of the strokes, they generate multiple random strokes and select the stroke most suitable. During rendering, the tone of a surface is determined and used to select the proper texture out of the Tonal Art Map. Hardware multitexturing is exploited to blend together multiple hatching stroke textures per face. A 6-way blending scheme allows for producing smooth tone and orientation transitions and for maintaining spatial and temporal coherence. They use a lapped texture [40] parameterization with overlapping patches oriented to the curvature of the object. Lapped textures are a mechanism for texturing an arbitrary surface geometry with the assistance of overlapping patches aligned to a tangential vector field.
In order to incorporate various rendering styles in the real time hatching approach, the arrangement pattern and visual properties of the strokes can be modified. The results achieved with this hatching technique are of high image quality and are rendered at interactive frame rates. Figure 5 shows an example hatching image of this technique.

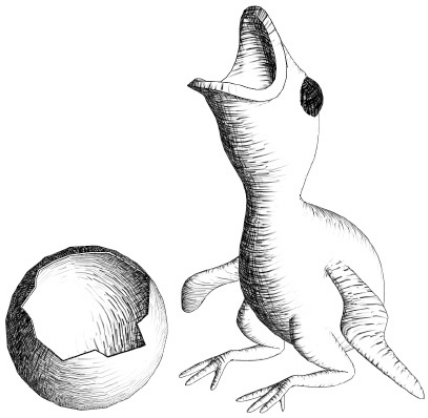

Figure 5: Real-time hatching of a $3D$ model. Image courtesy of Praun et al. [40].

Webb at al. [54] propose an extension of the technique described above. They enable a finer tone control and avoid artifacts existent in images of the former approach. An enhanced real time hatching according to Praun et al. [41] is performed on the GPU which allows for per pixel lighting, for using more tone levels, and for realizing the Tonal Art Map with volume texturing functionality. In addition to the increase of performance and amount of tone levels, using $3D$ textures allows for trilinear interpolation, which results in even smoother transitions. The images attained with this approach are of high quality. Results are shown in Figure 6.

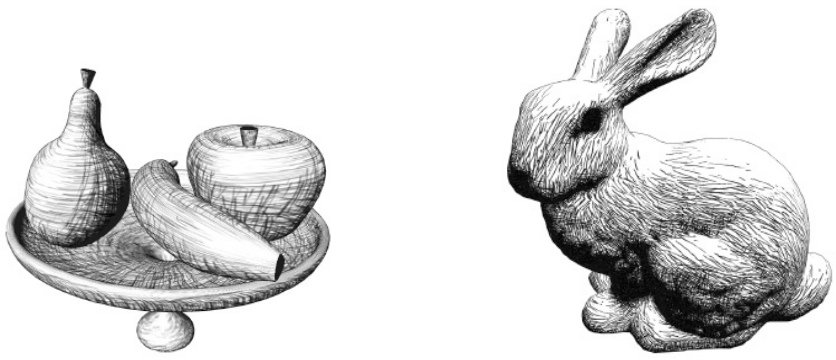

Figure 6: Fine tone control in hardware hatching. Images courtesy of Webb et al. [54].

Hertzmann and Zorin [18] present a technique for hatching free-form surfaces and polygonal meshes. They propose algorithms for silhouette extraction, cusp detection, and segmentation of silhouettes in smooth parts. Hatching strokes in a particular rendering style are created based on a smoothed direction field. For generating smooth hatching patterns, they detect quasi-parabolic regions and initialize the direction field using curvature directions from these regions. Then they optimize the direction field by propagating the attained directions to the remaining vertices. To create evenly-spaced hatching strokes following this direction fields they adapt the streamline placement algorithm of Jobard and Lefer [22]. Figure 7 shows example images of this approach.

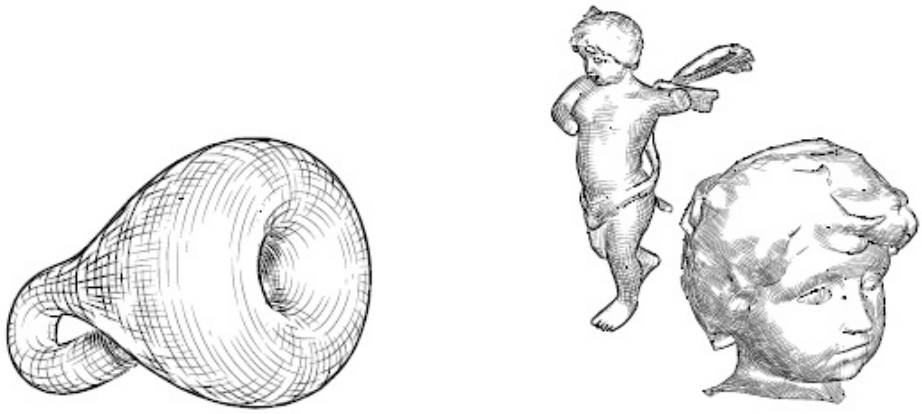

Figure 7: Illustrating smooth surfaces. Images courtesy of Hertzmann and Zorin [18].

Other high-quality results for pencil rendering of polygonal data are presented by Lee et al. [27]. In contrast to the techniques discussed above they shade the object with laminar pencil textures, not with hatching. Contours imitating the irregularities of hand-drawings are achieved by blending multiple slightly distorted contour images. Therefore, they perturb the contours by distorting the coordinates of a regular grid and afterwards use the distorted coordinates to render the contour. They draw multiple overlapping contour images with varying distortion via multitexturing.

They propose a method which eases mapping textures and aligning them to the curvature direction which does not use lapped textures. Pencil textures similar to Tonal Art Maps serve for communicating shape and tone. The pencil textures contain overlapping strokes in high density where individual strokes are not perceptible. For each face three textures with different orientations are blended together to align the texture to the principal curvature on a vertex basis. They furthermore use paper effects making the structure of paper become visible as graphite from a pencil does when applied on paper. When drawing a stroke, the difference between paper normal and drawing direction is used to darken areas where the drawing direction is opposite to the paper normal and to lighten areas where the directions are similar. Figure 8 shows result images of this pencil rendering approach.

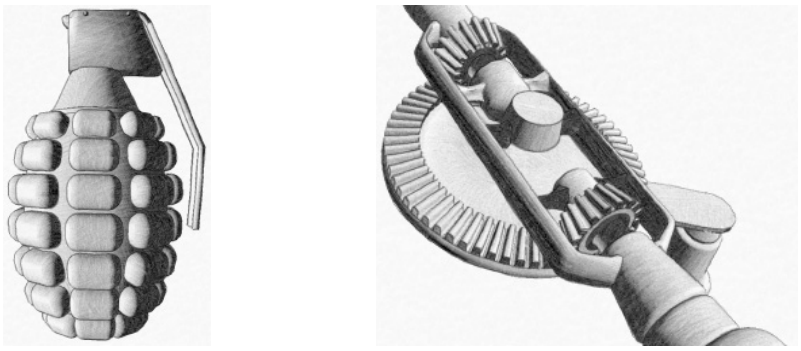

Figure 8: Real-time pencil rendering for polygonal data. Images courtesy of Lee et al. [27].

2.3 NPR in Volume Visualization

Non-photorealistic rendering methods are used in volume visualization due to their property of communicating visual information in a sparse, abstract form omitting irrelevant details while emphasizing critical aspects. Hand-drawn illustrations are used in many sciences for schematic representations or easy comprehensible imagery, for instance in teaching or textbooks. With the task of realizing such traditional illustration techniques with NPR methods, numerous approaches have emerged and will be outlined here. We start with discussing two-level volume rendering [17], an important work towards NPR in volume visualization. We continue with having a look at NPR methods involving a modified optical model to allow for transparency or alternative shading styles. Then we survey pen-and-ink rendering for volumes, which is a technique well suited for depicting scientific objects. Finally we present hatching techniques for volumetric datasets, which are the substance of this thesis.

2.3.1 Two-Level Volume Rendering

Two-level volume rendering [17] plays a crucial role in the evolution of NPR in volume visualization. In this work, Hauser et al. propose an approach which enables rendering subsets of a volumetric dataset in diverse styles. Different parts of the dataset are depicted individually with different rendering algorithms and are composed in a final merging step. This concept proves its strength when inner structures and semitransparent outer regions shall be rendered simultaneously, enabling a focus+context oriented visual representation. It also enables utilizing non-photorealistic shading or rendering models. This can be applied for example for rendering outer surfaces with an NPR line drawing technique while using a direct volume rendering algorithm for inner parts. The volume is rendered in two levels. One is the local level, on which each object is rendered individually and the other is a global level wherein all local levels are combined in the final compositing operation.
Rheingans and Ebert [11] also present the idea of combining realistic and non-photorealistic rendering techniques for volume illustration.

2.3.2 Volume Rendering with a modified Optical Model

In order to gain a stylized representation or to accentuate information transported with the image of the volume, visual properties of the depicted object such as color and transparency can be altered by involving an alternative optical model.
A hardware-accelerated approach for non-photorealistic volume rendering is presented by Lum and Ma [31]. They propose a mechanism for interactive expressive rendering and incorporate various NPR techniques such as tone-shading, silhouette rendering, gradient-based enhancement and color depth cueing. They use a $3D$ texture technique for GPU-based volume rendering. They exploit multi-texturing for realizing the different non-photorealistic effects with multiple textures. They use two rendering passes and store spatial information like gradients or silhouettes in four separate textures. Tone shading is used to convey lighting with color temperature or to discretize the tone spectrum. Their system includes silhouette extraction and illustration. Depth perception can be improved by modifying color depending on the distance to the viewer. By lightening and attenuating the color of distant structures, spatial relations can be perceived more easily. Figure 9 shows a result image.

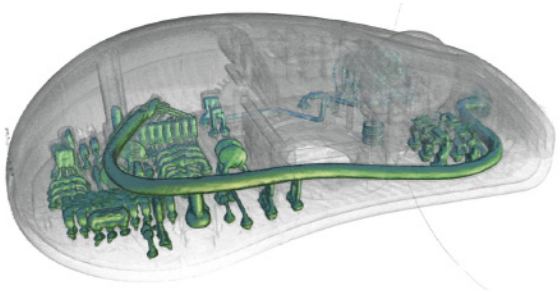

Figure 9: Hardware-accelerated non-photorealistic volume rendering. Image courtesy of Lum and Ma [31].

Another method for non-photorealistic rendering of volumes is proposed by Salah et al. [43]. They use it for illustratively rendering segmented anatomical data. The algorithm is based on surface points which are extracted as a subset of the segmented objects in an initial step. The shading is performed with halftoning, but the work focusses on silhouette extraction and rendition. Silhouettes are estimated via the normals corresponding to the surface points and the viewing position. The outlines are rendered using disks which are oriented to the normals so that the normals are perpendicular to the plane defined by the disk. These oriented disks result in ellipsoids in image space and their combination yields the impression of a hand-drawn outline consisting of multiple overlapping strokes.

Viola and Gröller [52] deal with the concept of smart visibility in visualization, which extends the transparency model of Diepstraten et al. [8]. They smartly uncover areas of high importance occluded by outer regions. One way to implement this is by reducing the opacity of objects occluding the important parts. Another way is by deforming or translating objects. This originates from technical illustration techniques denoted as cut-away views, ghosted views and exploded views. These techniques manage to emphasize and illuminate the most important information in a manner providing easy perception and visual harmony.

Viola et al. [53] propose importance-driven feature enhancement for smart visibility. In this technique, importance defines which objects ought to be clearly visible in the image. This importance is used to determine a priority the objects are tagged with. By mapping priority to a corresponding level of opacity or sparseness in the rendition, the abstracting effect of looking through irrelevant parts while the features of interest are pictured precisely and opaque can be achieved. Therein the own priority of the object as well as the priorities of occluding objects are taken into account. Figure 10 shows example images of this approach.

Figure 10: Importance-driven feature enhancement in volume visualization. Images courtesy of Viola et al. [53].

Viola and Gröller [52] survey some applications of visibility-altering approaches in visualization. Straka et al. [47] for instance apply a cut-away technique in CT angiography for revealing blood vessels which are typically occluded by other tissue. Krüger et al. [25] apply a smart visibility method in neck dissection planning for making lymph nodes hidden by opaque tissue become visible and emphasizing them. Instead of using transparency, other possibilities of revealing certain objects in volume rendering are offered by deformations and geometric transformations of the volume data. These methods alter the spatial properties of the depicted object. One approach [5] distorts the data in a way that important features gain more display space. Another technique is called volume splitting [21] and allows for displaying multiple iso-surfaces concurrently. Each iso-surface except the innermost one is split into two parts. The two halfs are then moved apart to uncover the object of high importance. Ghosted views render selected and spatially transformed objects at their original location as well as their transformed representation.

2.3.3 An Interactive System for Illustrative Visualization

VolumeShop, an interactive system for illustrative visualization, is presented by Bruckner and Gröller [2]. This hardware-accelerated application allows for interactive creation of illustrations from volumes based on scientific and technical illustration conventions. The system allows for multi-object volume rendering where visual properties of intersections between objects can be defined via a two-dimensional transfer function.

VolumeShop additionally offers different non-photorealistic shading models such as cartoon and metal shading. It enables interactive selection with a three-dimensional painting method.
Bruckner and Gröller use selective illustration techniques for focus+context visualization. Cutaway views and ghosting can be achieved as well as importance-driven volume rendering for smart visibility according to Viola et al. [52]. Illustrative context-preserving volume rendering [1] is performed for simultaneous visualization of interior and exterior structures.
To indicate the role of an object in the image, illustrators follow certain visual conventions. VolumeShop offers various kinds of visual enhancements based upon this conventions. One is to display the bounding box of an object which provides clues for spatial perception. Another method is using an arrow for showing the translation between the transformed selection and its original position. Fanning is a technique for emphasizing objects by displaying a connected pair of shapes. Furthermore, annotations describing the content of the volume verbally can be displayed. Figure 11 shows a result of this illustration system.

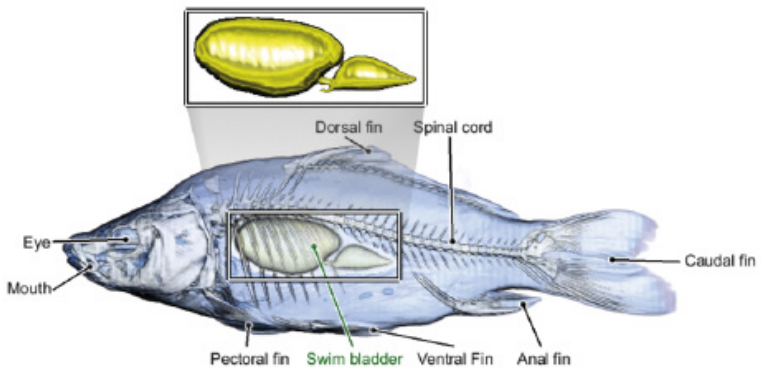

Figure 11: VolumeShop: An interactive system for volume illustration. Image courtesy of Bruckner and Gröller [2].

2.3.4 Line Drawings from Volume Data

Burns et al. [3] develop a technique for directly extracting and rendering silhouettes and suggestive contours [7] of volumetric data. They suggest a seed-and-traverse algorithm for contour extraction. Initial seed points are detected with the help of an equation for iso-surface and contour definition. Once a contour-containing surface voxel is determined based on this equation, the contour is followed using a variant of the marching lines algorithm [50]. In order to bypass the need for examining all voxels, they utilize a seed-and-traverse algorithm denoted as walking contours. Starting with an initial seed they perform a marching lines search along the silhouette until returning to the initial seed. During animation, adequate seed points from the previous frame are re-used exploiting spatio-temporal coherency of contour lines. New seed points are found in random cells using a gradient approximation for determining if the cell contains a contour. For comprehensible rendering, they distinguish between different families of lines such as silhouette lines or suggestive contours and depict them in differing rendering styles. Line visibility is computed using raycasting.

2.3.5 Pen-And-Ink Rendering in Volume Visualization

As pointed out before, pen-and-ink drawing is a popular illustration technique due to the degree of abstraction achieved in its pictorial representations. A psychological study with architects [45] showed that pen-and-ink imagery often is preferred to a realistic one. Therein architects were asked to compare computer generated sketches against realistic CAD images and generally favored the hand-drawn style images. Treavett and Chen [51] present pen-and-ink illustration techniques for volume visualization. They introduce a $3D$ drawing and a $2^{+}D$ drawing method. Within the $3D$ approach three-dimensional strokes are created in object space and then projected onto the image plane. A general definition of NPR textures is made by defining an NPR texture as a filter:

$$F(p, O_{att}, T_{att}) \rightarrow \{opacity, color\}$$

Here p is a point in texture space, O_{att} are object attributes correlated with p and T_{att} is a set of texture attributes. They use $3D$ textures to create the three-dimensional strokes. They suggest an approach that renders the volume in two passes. One is for lighting computation with traditional volume rendering mechanisms. The other rendering pass serves for the creation of the three-dimensional strokes using the intermediate volume rendering output as input.
Treavett and Chen further suggest a 2^+D approach applying two-phase rendering. In the first phase all relevant information about the object is gathered in object space and stored in dedicated image buffers. The second phase is used for creating strokes in image space. The particular renditions are then composed in an amalgamation step to produce the final image. This is referred to as a 2^+D technique because $2D$ image elements are created using $3D$ information. The intermediate images serve to determine visual properties of the pen-and-ink drawing. Outlines can be extracted with the help of the distance variation between adjacent pixels or the angle between viewing direction and gradient. The length, thickness and density of the strokes can be controlled in dependance of the lighting. Strokes can be oriented along the curvature of the rendered object. This 2^+D concept was adopted for the volume hatching method developed in this thesis.
Figure 12 displays example images of this approach.

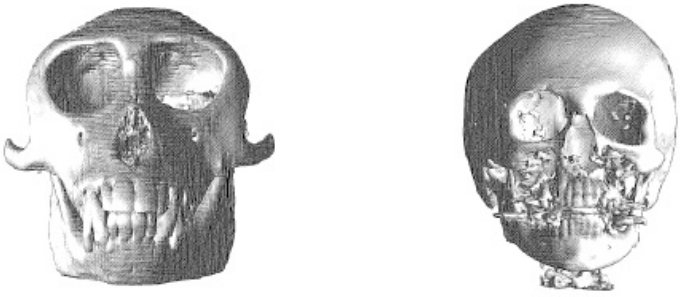

Figure 12: Pen-and-ink rendering in volume visualization. Images courtesy of Treavett and Chen [51].

2.3.6 Volume Hatching

We now have a look at two hatching techniques for volumetric data. One was presented by Nagy et al. [38] together with fragment shader implementations of toon shading and silhouette rendering for volumes. The hatching is created in two passes. In the first pass a hatching direction field is set up by computing higher order differential characteristics like curvature and storing them in a hierarchical data structure. The second pass serves for creating three-dimensional strokes in object space coinciding with this hatching field and rendering them as line primitives. In order to access curvature data efficiently they encode it into an octree representation. For the creation of hatching strokes seed points indicating the start position of the strokes are distributed in the volume. Initial seed points are determined with a data driven placement method. Therefore the octree structure is traversed using scalar values and curvature information to decide whether seed points have to be inserted in the current cell. The octree allows for efficiently skipping empty regions, planar areas and structures specified to be transparent. The number of seed points is chosen in dependance of normalized gradient magnitude and mean curvature information. They position a larger amount of seeds in areas of high curvature and place seed points more sparsely in homogeneous areas. The seed points are initially placed in the center of the cells and then shifted towards iso-surfaces. For hatching the object a subset of this pre-computed seed point set is selected during runtime and a three-dimensional stroke is created for each selected seed point. A path following the principal curvature direction is traced in object space. A stroke is stored as a set of points and rendered using line primitives. The direction field is numerically integrated employing a Runge-Kutta integration with adaptive step size. The strokes are rendered as line strips enhanced by anisotropic line shading. In addition to that Nagy et al. determine whether a part of a stroke depicts a front facing or a back facing part of the surface and use this information to color the strokes respectively. By using different colors for front and back facing regions they implement two-sided lighting. Furthermore cross-hatching of dark regions is performed using the minimal curvature direction. The concept of pre-computing strokes in object space and the graphics hardware

implementation of rendering routines allow for rendering large-scale volume datasets on consumer class hardware at interactive rates. The images generated with the method of Nagy et al. have an artistic appearance of high expressiveness and visual attraction. Spatial perception is enhanced by their two-sided lighting approach and volumetric hatching. Figure 13 shows example images from their approach.

Figure 13: Volume hatching examples. Images courtesy of Nagy et al. [38].

Another volume hatching approach was presented by Dong et al. [10] for non-photorealistic rendering of medical volume data. They suggest a volumetric hatching pipeline consisting of a separate determination of silhouette points and stroke generation in the first step. This information is then drawn by a dedicated rendering module. The silhouette points are detected in object space via comparison of voxel positions along viewing lines cast into the volume. The three-dimensional contour points are then projected into image space and connected to silhouette lines. A visibility determination is performed during the projection. The projections are connected with straight lines and result in rather smooth outlines if a sufficient density of silhouette points is given. In order to remove redundant contour information some points in areas of high silhouette point density are removed.
Computation of stroke directions is done by either a method dedicated for detecting muscle fiber orientation [9] or by curvature estimation. The muscle fiber orientation approach is suited for displaying organic properties of muscle tissue. Using the principal curvature direction for stroke orientation is universally applicable. Dong et al. hereby use the method of Thirion and Gordon [49] for estimating partial derivatives.

A stroke is produced by fitting a local surface patch which approximates the objects shape and by intersecting this patch with a normal plane following the stroke direction. This intersection defines a three-dimensional stroke. During rendering illumination is performed in object space by determining the voxels' lighting intensity and mapping it to the number of associated strokes to be drawn. Only strokes within the shell defined by the transfer function are selected for rendering.
The results presented by Dong et al. are of a rather high visual quality, but their method suffers from the drawbacks of limited silhouette accuracy and smoothness, the need for segmentation because of its object-based nature and low computational performance. Figure 14 shows example images.

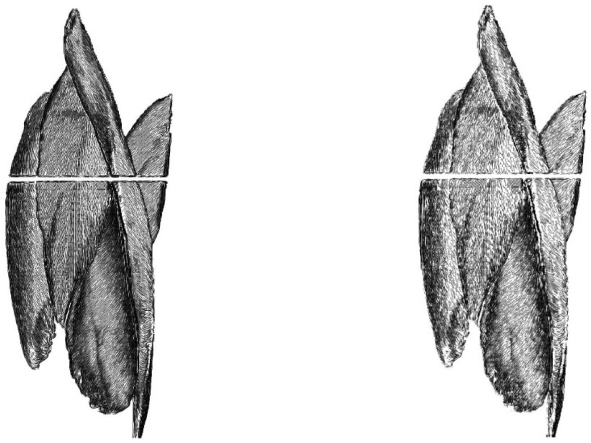

Figure 14: Volume hatching examples. Images courtesy of Dong et al. [10]

2.4 Curvature Estimation in Volume Visualization

In order to integrate higher order differentials into the transfer function, Kindlmann et al. [23] suggest a method for direct curvature estimation. This technique was adopted for curvature computation in the volume hatching system developed in this thesis. In volume hatching, curvature direction can be used for aligning hatching strokes to the object's shape. The first-order derivatives of the scalar values make up the gradient vector, which approximates a surface normal. The gradient is used for illumination, visibility and silhouette computation in volume visualization. Curvature is defined through the second-order derivatives of the volumetric function. It represents the variation of surface normals. Kindlmann et al. employ a convolution-based approach for measuring the curvature and suggest three simple implementation steps for realizing it. This technique is based on a tangent space projection of the Hessian matrix. Various filtering techniques are examined for reconstruction and experiments result in the statement that a B-spline-based convolution is well suited for curvature estimation.

Kindlmann et al. introduce the concept of thickness-controlled contours. Herein the normal curvature along the viewing direction is used to modulate the width of contours in the volume contour rendering. This can be used for rendering contours of consistent and controllable width avoiding that contours become thicker in low-curvature regions. Contours with varying width appear if just the gradient and viewing direction are used for contour computation.

2.5 Evenly Spaced Streamlines

Jobard and Lefer [22] present an approach for creating evenly-spaced streamlines of arbitrary density for $2D$ flow visualization. We adopt this technique to create hatching strokes oriented along the principal curvature direction for volume hatching. Given a $2D$ vector field, their method creates equidistant streamlines. The algorithm allows to control the separating distance between the streamlines to modify the appearance of the flow field visualization. The generation of a streamline is stopped if the distance of a new candidate point to any other streamline is lower than the specified separating distance. Additional break conditions are reaching a singularity in the vector field or the border. For streamline creation they start with an initial seed point and trace the vector field in two opposite directions. Further candidate seed points for streamlines are derived from existing ones at the separating distance. Figure 15 shows an example of evenly-spaced streamlines.

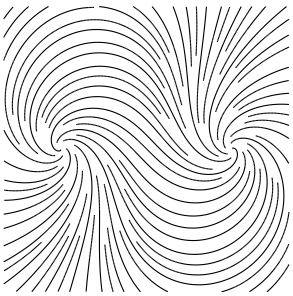

Figure 15: Evenly-spaced streamlines in a $2D$ vector field. Image courtesy of Jobard and Lefer [22]

3 Volume Hatching

In this chapter we present the techniques developed for rendering images of volume datasets which resemble hand-drawn hatchings. We start with explaining the rendering pipeline of our volume hatching system. Then a survey of the system which is used for depicting contours with a hand-drawn appearance is given. We continue by explaining the method we employ for rendering stylized strokes. Afterwards we address curvature estimation which is used for hatching stroke orientation. Then we outline some experimental approaches which emerged while searching for a strategy for volume hatching. We proceed with discussing our final approach to volume hatching based on streamlines. Finally we describe the way we enable volumetric hatching.

Figure 16 shows the conceptual architecture of our rendering pipeline. Contour drawing procedures are displayed on the left, hatching procedures on the right side.

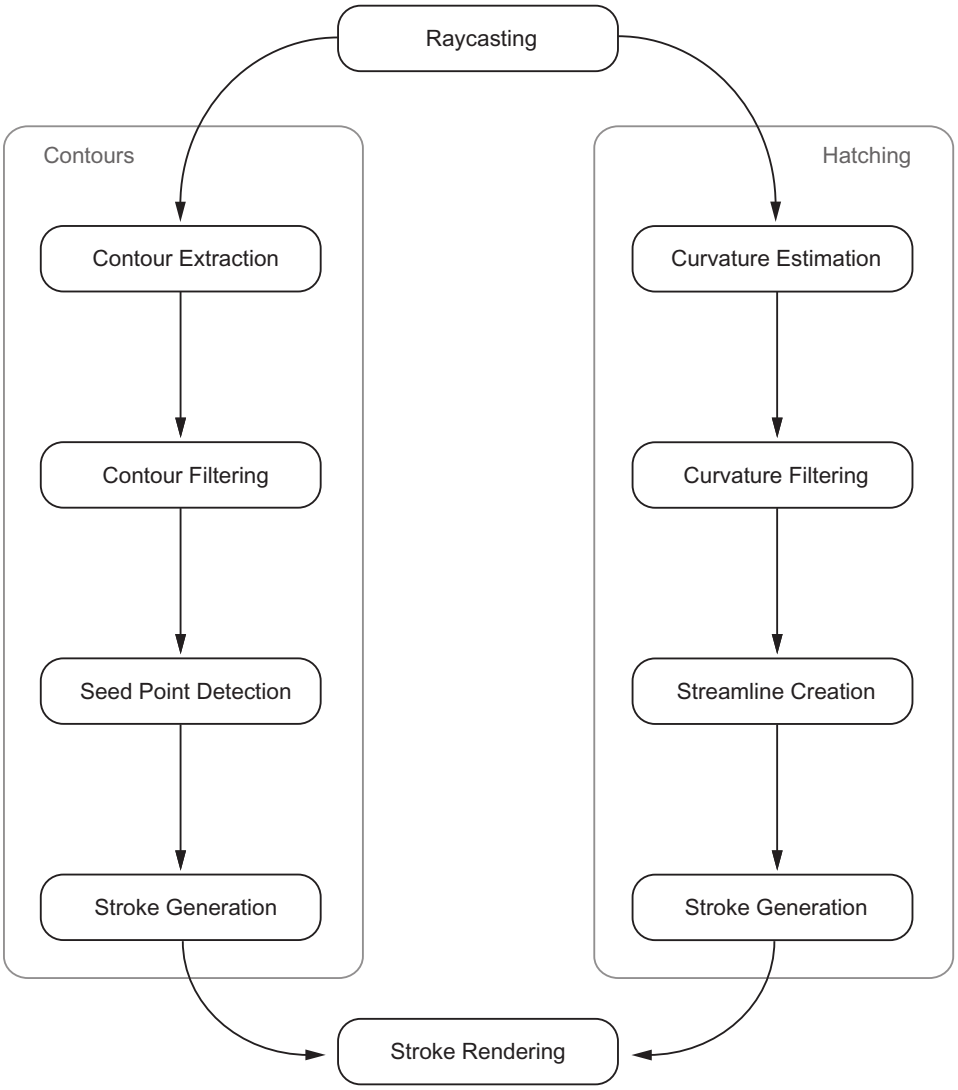

Figure 16: Schematic illustration of the volume hatching rendering pipeline.

The input to the volume hatching pipeline is a volume dataset, its output is an image consisting of contour and hatching strokes. Contours and hatching strokes are created separately and merged for the final image. The first step in the pipeline is a raycasting procedure. For samples at the first ray-object intersection, optical and spatial properties of the rendered object are computed and stored in $2D$ textures. We subsequently use this information to determine the adequate placement and orientation of strokes.
For contour drawing the required information to be generated during raycasting is information on contour locations (see Section 3.1.1). The input for this operation is the volume dataset, the output is a $2D$ contour texture. In a preprocessing step this contour information is filtered (see Section 3.1.2) and the output is the filtered contour texture. Then seed points on the contour are detected with a line-following algorithm (see Section 3.1.3). This operation gets the filtered contour texture as input and generates an array of contour points as output. Afterwards strokes are generated from this set of contour points (see Section 3.1.4), yielding an array of strokes as output. Each stroke is defined by a number of control points. Finally the contour strokes are rendered (see Section 3.2).
For the hatching strokes the reference information to be generated during raycasting is information on lighting intensity and curvature direction (see Section 3.3). The output of the raycasting operation are two $2D$ textures containing this information. Curvature information is smoothed in a preprocessing operation (see Section 3.3), which outputs a filtered curvature direction texture. Then streamlines are created using the curvature direction image as input (see Section 3.5.1). The output of this operation is a set of curvature-aligned streamlines. Simultaneously to creating streamlines, hatching strokes are generated by extracting them from the streamlines (see Section 3.5.2). Output of this operation is a set of hatching strokes. Each stroke is defined by an array of control points. Streamline generation and stroke extraction are repeated to produce hatching (see Section 3.5.4) and crosshatching layers (see Section 3.5.5). Subsequently hatching strokes are rendered (see Section 3.5.3).

3.1 Contour Drawing

In the following we explain the algorithms we use for extracting and rendering contours in a visually pleasant manner. The majority of NPR techniques depict contours using simple rendering methods. Although sophisticated silhouette extraction mechanisms have emerged, the rendering of silhouettes is mostly done using line primitives or just black color for contour pixels. If only contours are drawn this might not be a problem. As soon as contours are drawn in combination with hatching using a different rendering style it affects image quality. It conveys the impression of hatching an object with a pencil and drawing its contours with another drawing medium, for instance pen-and-ink. In contrast to that, we developed an approach for stylized contour depiction. It is based on a simulation of the human hand-drawing process and allows for rendering both contours and hatching with identical visual appearance. When a pencil drawer creates the outline of an object, he draws multiple overlapping strokes for approximating the silhouette and refines it incrementally. This can result in a sketchy visual appearance when the contours are drawn fast or in a smooth and precise appearance where individual strokes are no longer recognizable. As this thesis is concerned with generating imagery with a hand-drawn appearance, we try to mimic the hand drawing process by depicting multiple strokes following the contours. Strokes are not drawn as line primitives. A stroke is depicted by a brush texture drawn along a spline, which enables smooth strokes and various stylization. Our contour drawing mechanism consists of four steps. Initially, silhouette extraction is performed during raycasting (see Section 3.1.1). Afterwards the contours are filtered (see Section 3.1.2). Then we use a line-following algorithm to sequentially find points on the contour (see Section 3.1.3). Finally, subsets of these points are selected and used as spline control points for drawing contour strokes, as described in Section 3.1.4.

3.1.1 Contour Extraction

Detecting contours is performed during volume rendering. We use the angle between gradient and viewing direction as a criterion for silhouette extraction. It is based on the fact that contours lie in regions where a surface is perpendicular to the viewing direction. These are regions where the dot product between view vector and gradient yields a small value. We additionally implement the concept of thickness-controlled contours suggested by Kindlmann et al. [23]. Applying this method is advantageous for our line-following algorithm. Without thickness-controlled contours, planar areas result in thick contours. When tracing thick contours, our line-following algorithm generates adjacent contour points in a zigzag arrangement of high density, because too many adjacent contour locations are detected.

The contour detection is done at the positions of the first ray-object intersections, which define the outer shell of the volume. We additionally compute the image-space direction of the contour through the cross product between viewing direction and gradient. As we use a GPU raycaster for volume rendering, all these contour extraction routines can be performed efficiently in graphics hardware. Contour information is stored in a dedicated texture image. Figure 17(a) shows a contour image generated with the described methods. The color coding uses green for contours in x direction, blue for contours in y direction and alpha for the contour value.

3.1.2 Contour Filtering

To improve the results of our line-following method for finding control points on the contour, we filter the contour image in a preprocessing step. We employ a Gaussian convolution in order to eliminate noise and close gaps. As contour points are detected by sequentially finding adjacent positions on the contour lines, the line-following algorithm would stop at gaps in the contour. It stops because no new adjacent contour position can be detected at such positions. Most of these gaps are closed by Gauss filtering the contours, so the line-following algorithm can generate longer sequences of contour seed points.

The other advantage of filtering is that noise in the contour image is eliminated. Noise is generated during contour extraction at small separated areas representing a contour location. These areas are not connected to the main contours and result in separated dots in the contour image. In Figure 17 these dots are noticeable on the back of the stagbeetle. It is not desired to draw a contour at these locations. In addition to this, these separated locations can be falsely connected to the main contours during line following if they are nearby. Gauss filtering the contour image eliminates most of these separated contour locations.
We separate the Gauss convolution to reduce the number of instructions. Experimental results have shown that a filter kernel size of three and one filtering pass are best suited for our needs. Filtering the contour image too intensively leads to a thickening of the contours. During line following for seed point detection, this results in the effect of too many adjacent contour seed points, as described in Section 3.1.1. The convolution is done on the GPU. Figure 17(b) displays a contour image filtered with this method.

(a) (b)

Figure 17: Contour image of stagbeetle, (a) without and (b) with Gauss filtering. Color encodes contour direction.

3.1.3 Seed Point Detection

In order to detect seed points on the contours in a partially sequential order, we employ a recursive line-following algorithm. It starts with finding initial points which serve as start points for following the lines. We need multiple start locations for sampling all silhouette lines which are possibly unconnected. The start points are detected using horizontal and vertical equidistant scanlines. These scanlines are traversed in left-to-right respectively bottom-to-top order, checking if the corresponding contour values exceed a dedicated threshold. If a contour location is detected, a start point is generated and a small number of successive pixels on the scanline is skipped in order to avoid setting multiple start points at nearly the same contour position.
Figure 18(a) shows the start points obtained with this scanline approach.

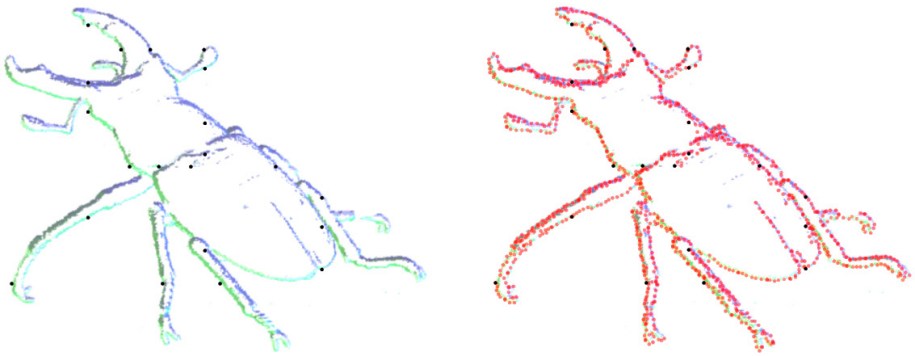

(a) (b)

Figure 18: Contour seed points, (a) initial points as black dots and (b) points detected with line-following algorithm as red dots.

Once the start points are detected, we apply a recursive line growing algorithm from each start point. This algorithm is illustrated in Figure 19. The the red lines represent contours and the grid represents pixels. Green pixels are newly detected contour locations, blue pixels formerly detected ones. The actual pixel position is marked with a blue outline.

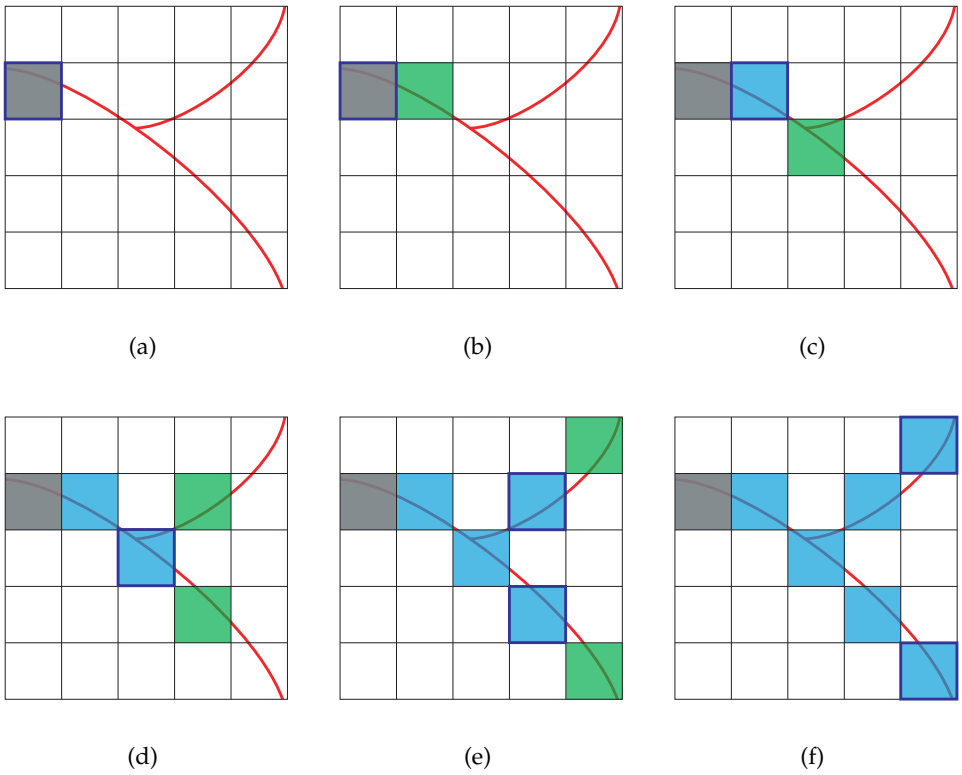

Figure 19: Illustration of the line-following algorithm for contour point detection.

In 19(a) a start position on the contour is depicted as a grey pixel. At this location we search the local neighborhood for the two adjacent pixels with the highest contour value. We detect two locations in order to continue in two directions at locations where the contour branches. At the start location in 19(a), only one adjacent contour pixel is detected, this detection is depicted as a green pixel in 19(b). We recursively continue at the new position. In 19(c) the contour pixel detected next is again depicted in green, the pixel found before is depicted in blue. With the new location in 19(c) the algorithm reached a branching position. As depicted in 19(d), two new locations are found. The algorithm continues with tracing the contours from these two positions. In 19(e) adjacent contour pixels are found on both branches. The entire contour has been traced in 19(f).
We recursively continue this region growing algorithm until no new contour position can be detected. We need to remember the already examined

locations in order to proceed along the contour lines and to provide a stopping condition for the recursion. The examined locations are marked with the help of a boolean field.
When the recursion stops contour points are seeded in fixed intervals during backtracking. This mechanism yields points on the contour in equal distances. These contour seed points are stored in an array. In Figure 18(b) the contour points obtained with the described algorithm are shown as red dots. The black dots are the start points obtained with the scanline approach. Contour points traced from the same start point are gained in sequential order. This partially-sequential organization of points eases the selection of control points appropriate for a spline representation.

3.1.4 Stroke Generation

We now discuss how control points for splines used for drawing silhouette strokes are selected from the set of partially-sequential contour points. As mentioned previously, strokes in the contour drawing should overlap. The stroke generation method for a sequence of contour points is illustrated in Figure 20.

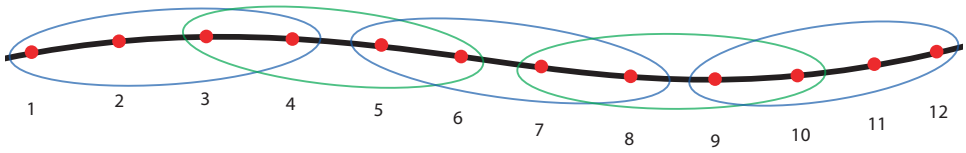

Figure 20: Schematic illustration of contour stroke generation for a sequence of contour points.

Herein the black line is a contour line and the red dots are contour seed points. The numbers represent the storage order in the contour seed point array. The ellipsoids each mark a set of points which is selected to form a stroke. In this illustration, each stroke is generated with four control points. A new stroke is generated at an offset of two points in the point array. In this way we realize the overlapping of strokes.

Because our contour points are not stored entirely in sequential order, we include two constraints during stroke generation. The first constraint is a maximum distance between seed points. We illustrate this in Figure 21.

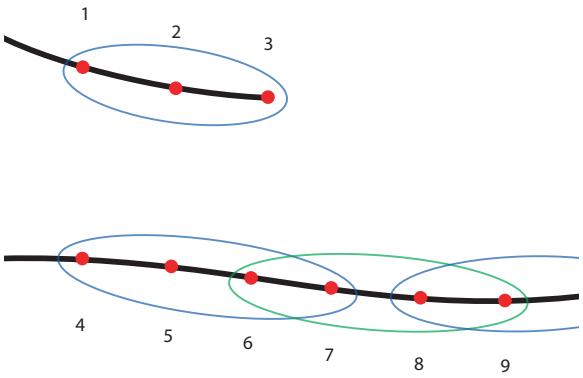

Figure 21: Schematic illustration of contour stroke generation. The first stroke is completed at point 3 because the distance to point 4 exceeds a maximum distance threshold.

Here two contour lines are depicted. The upper contour line ends at the position of seed point number 3. The following points in the contour seed point array (4,5,..) are placed on another contour line. This is a result of using scanlines for start point detection and storing all points in one array. It is not desired to connect seed points number 3 and 4 to form a stroke. We circumvent this by checking the distance between the actual point (3) and the next point in the array (4). If it exceeds a maximum distance threshold, we end the current stroke. Seed points 1, 2 and 3 are used as control points for one stroke. A new stroke is initialized at position 4. From this position, the following points are again sequential and strokes are created as explained in Figure 20.
The second constraint included during stroke generation is the contour direction. We obtain this direction via the cross product of viewing direction and gradient. The selection of control points for a stroke stops if the contour direction of the new point differs too much from the actual point. We illustrate this situation in Figure 22.

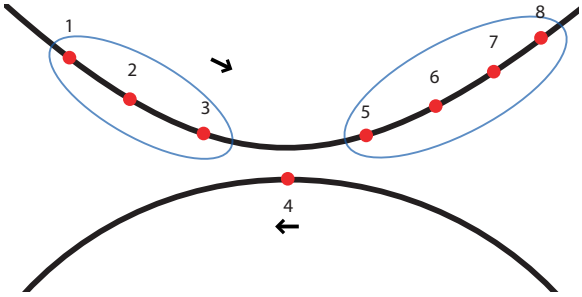

Figure 22: Schematic illustration of contour stroke generation. First stroke is completed at point 3 because contour direction of point 4 differs too much.

This figure shows two adjacent contour lines. While tracing the upper contour line, our line-following algorithm has detected seed point number 4 on the other line below. This is a result of the convergence of the two contour lines. We do not want to connect seed points number 3 and 4 to a stroke. We avoid it by taking into account the contour direction at these positions. The contour direction is depicted with the arrows. Because the contour direction at point 4 differs too much from the direction at point 3, we stop the control point selection at point 3. A new stroke is created beginning at point number 5.

To realize the described constraints, we use splines with a variable number of control points. The maximum number of control points per spline is set to 16. Contour stroke generation stops when the entire array of seed points is traversed.

To achieve a hand-drawn visual appearance, the contour-depicting splines can be geometrically randomized. One way is to perturb the control point positions by adding noise. Bending of a stroke can be achieved by displacing an arbitrary control point and propagating this displacement to the other control points. Another way is lengthening contour strokes by displacing the last control point in contour direction. This causes individual contour strokes to become more perceptible and a sketchy outline effect can be achieved. Furthermore, applying a slight random rotation and translation before drawing each stroke also yields this effect. Our approach allows for numerous visual modifications and for mimicking manual contour drawing. Results of our contour drawing approach are shown in Figure 23.

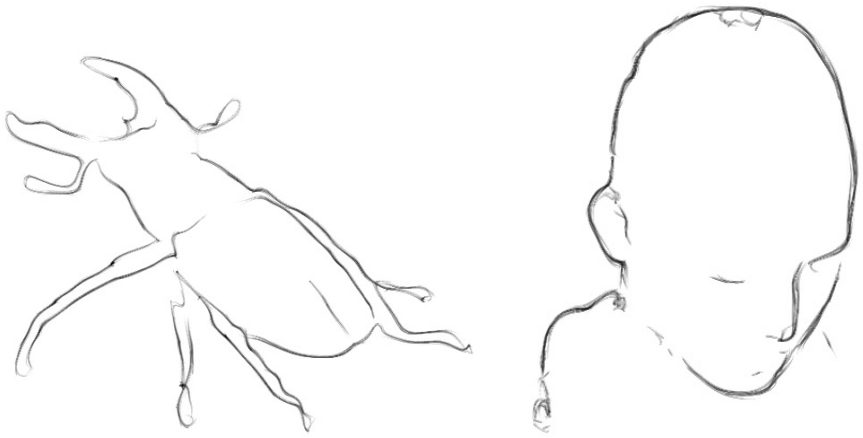

(a) (b)

Figure 23: Contour drawings of (a) stagbeetle and (b) human head.

Our mechanism does not create completely accurate and precise contours. It produces squiggles and slight deviations from the exact silhouette. This is a result of errors in the line-following and control point selection mechanisms. We argue that this randomness enhances the hand-drawn appearance of the silhouette rendering. Other techniques compute precise line information and intentionally add deviations afterwards to achieve such effects. Our algorithm generates such deviations inherently. However, the randomness of our contour renderer is misleading and disturbing in some cases. If a precise contour drawing is desired, we offer the possibility to display the extracted contour image directly.

3.2 Stroke Rendering

In this section we will discuss our method for drawing strokes as textured splines. We employ this method for both contour and hatching strokes to achieve the same visual representation for these basic image elements. In comparison to drawing line primitives, as many stroke-based rendering approaches do, it allows for a stylized rendition of the strokes. In order to enable drawing smooth strokes of arbitrary shape we choose splines as a basis for our stroke rendering technique. Each stroke is drawn along a spline defined by a number of control points. Following brush-based drawing, which is commonly used in drawing applications, we blend multiple overlapping quads bearing a brush texture along a curve. Using this method we can easily change the drawing style for simulating various artistic drawing media by using different brush textures. Figure 24 shows some brush textures integrated in our volume hatching system.

Figure 24: Different brush textures to be used for generating various stylization.

Width and opacity of the textured quads are increased at the beginning of the stroke and decreased at its end. In this manner we realize tapering and fading in and out of the strokes. The opacity of hatching strokes is altered according to the lighting intensity. Randomly modifying size and opacity of the quads to be drawn can be used for adding randomness to the strokes. The stroke rendering algorithm determines the number of quads per stroke depending on its length. For each quad, it computes position on the spline as well as size and opacity and draws it using $2D$ texturing and alpha blending. This method offers many possibilities for adding irregu-

larities and for individualizing strokes. These possibilities are not given if only one texture is used for the entire stroke. In Section 3.1.4 it is described how strokes can be geometrically randomized. Furthermore, drawing each stroke individually implies higher irregularities than texture-based hatching approaches. This leads to a less artificial and computer-generated visual impression.
In order to limit computational cost, we use simple Bézier splines. These curves can easily be computed with the algorithm of De Casteljau. The fact that Bézier curves are approximating, not interpolating splines is not of crucial importance due to the fact that we define rather short splines with a high number of control points. The curves are almost interpolating. Although our approach involves drawing a high amount of geometry for rendering, we did not observe a critical impact on performance. Figure 25 displays a single stroke rendered with our stroke drawing mechanism.

Figure 25: A single stroke rendered as textured spline.

3.3 Curvature Estimation

We approximate curvature information to align hatching strokes to the surface of the rendered object. This is advantageous for displaying spatial properties of the dataset. We use the method of Kindlmann et al. [23] to estimate curvature information (see Section 2.4). We use the following expressions:

1. $n = -g/|g|$, where g is the gradient.
2. $P = I - nn^T$, where I is the identity matrix.
3. $G = -PHP/|g|$, where H is the Hessian matrix.
4. $T = trace(G), \quad F = frobeniusnorm(G)$
5. $\kappa_1 = \frac{T+\sqrt{2F^2-T^2}}{2}, \quad \kappa_2 = \frac{T-\sqrt{2F^2-T^2}}{2}$

Therein κ_1 is the principal, κ_2 the secondary curvature magnitude. Principal curvature direction and magnitude of a sample on an iso-surface are computed in the fragment shader and stored in a $2D$ texture. We obtain the Hessian matrix by determining central differences of pre-computed gradient vector components. Curvature magnitude values are represented as eigenvalues of G. Determining the curvature directions requires computing the eigenvectors corresponding to κ_1 and κ_2. This requires solving a linear equation system. We employ Gauss-Seidel iteration, which is also suitable for fragment shader implementation. We use four iterations to approximate the solution of the equation system.
After rendering curvature information to dedicated textures, we smooth this data by performing a Gauss filtering. We use a convolution kernel weighted with the curvature magnitude to implement a filtering sensitive to the degree of curvature. In analogy to the filtering of contour information (see Section 3.1.2), we use a separated filter. We apply multiple Gauss filtering passes in order to smooth curvature directions in a way that they are suitable for obtaining smooth hatching strokes. If the curvature direc-

tion is not smoothed properly, curvature irregularities result in discontinuous strokes and the variation between hatching stroke directions is too large. Furthermore the filtering operation is necessary to avoid hatching too many details of the depicted object. We observed that the computation of the second-order derivative information does not critically decrease the performance of our volume renderer. Figure 26 displays curvature textures gained with the methods described above. The principal curvature direction is mapped directly to the color vector: curvature x direction is encoded in the red, y direction in the green and z direction in the blue color channel.

(a)

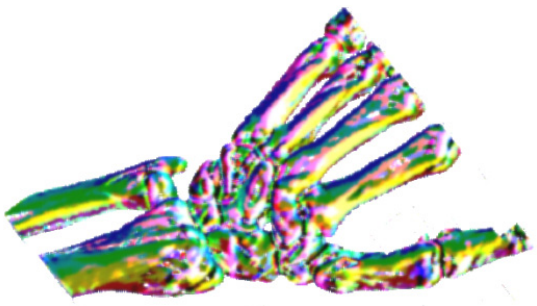

(b)

Figure 26: Principal curvature direction textures of (a) stagbeetle and (b) hand dataset.

3.4 Volume Hatching Experiments

In the following we will outline earlier strategies we tried for generating hatching images from volumes. The first experiment used a three-dimensional lighting transfer function to create strokes. The second experimental approach was concerned with applying a hatching technique for polygonal data to volume rendering. Then we decided to follow a 2^+D approach based on rendering each hatching stroke individually and tested a quadtree-based stroke placement before settling on our streamline-based approach.

3.4.1 Hatching using a Lighting Transfer Function

Bruckner and Gröller [2] use a two-dimensional lighting transfer function in VolumeShop to realize various lighting models, silhouette enhancement and to emphasize intersections of different objects. One experimental approach for volume hatching basically extends this two-dimensional lighting transfer function into the third dimension. The third dimension is accessed according to curvature magnitude. Black slices in this transfer function serve to render pixels of equal curvature magnitude in black. In this manner we produced black curvature-aligned strokes within the volume rendering. The problem with this approach is that it is only applicable for synthetic datasets with very smooth surfaces. Curvature irregularities in real-world datasets rather result in irregular sets of dots instead of strokes. We therefore decided to try other methods for realizing volume hatching. However, we got a stippling renderer as a byproduct of this experiment. We generated a three-dimensional lighting transfer function which contains dots instead of black slices. The density of dots was set appropriately to cover areas of high curvature and low lighting intensity with denser stipples. Figure 27 shows a result image of this method.

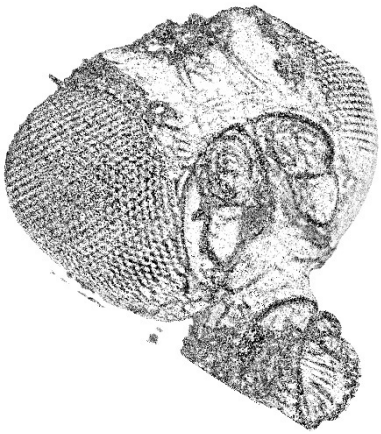

Figure 27: Volume stippling of a fly's head generated via three-dimensional lighting transfer function.

3.4.2 Applying Tonal Art Maps to Volume Rendering

The next approach we tried is based on the work of Praun at al. [41] (see Section 2.2.3). It is a texture-based technique for producing hatchings of polygonal data. We tried to apply it to volume rendering. This includes rendering a grid of overlapping quads aligned to the image plane as a counterpart to the lapped textures parameterization [40]. Tonal Art Maps are created as proposed in the work of Praun et al. [41]. They are selected depending on lighting intensity and oriented on the overlapping geometry according to curvature information and object transformation. This is where we encountered problems with this approach. The orientation of the textures can be aligned to the projected curvature directions, but realizing $3D$ transformations properly in $2D$ texture space is the principal problem of this approach. We did not find a way to realize object space rotations with adequate $2D$ texture space transformations. Furthermore, it is difficult to communicate local properties, such as per-fragment curvature, with global methods, by means of rendering multiple fragments with one textured primitive.

3.4.3 Quadtree-Based Stroke Seeding

Due to the problems we met with the texture-based approach mentioned in Section 3.4.2, we tried a mechanism which allows for better taking into account local properties. We generated each hatching stroke individually instead of using textures containing multiple strokes. We had lighting intensity and curvature direction information ready for placing and orienting hatching strokes. The difficulty was to find an appropriate seeding strategy for placing the strokes. They have to be somehow evenly distributed and placed according to the brightness.

The first mechanism we explored uses a quadtree constructed dependent on the lighting intensity. Stroke seed points are placed within the quadtree nodes while the corresponding lighting intensity and size of the node defines the amount of strokes contained. We generate stroke seeds according to a pseudo-random distribution to achieve inter-frame coherence.

The limitation of this approach is that it is capable of generating equally distributed stroke seed points according to the lighting intensity, but does not ensure that the strokes are evenly spaced. As we just seed points, which are used as stroke start positions, and not strokes themselves, this approach does not provide strokes which are equidistant along their entire length.

3.5 Streamline-Based Volume Hatching

Searching for a method for placing equidistant, curvature-aligned strokes in image space, we applied Jobard and Lefer's technique [22] for creating evenly-spaced streamlines. It is a $2D$ flow visualization method and creates equidistant lines following the directions specified by a $2D$ vector field (see Section 2.5). In this section we first present how we adopt Jobard and Lefer's algorithm for our problem. Afterwards, we discuss a technique to extract strokes from a set of streamlines. We draw the strokes as textured splines. Then we explain how we use multiple streamline sets to create hatching layers representing regions of different lighting intensities.

3.5.1 Creating Evenly-Spaced Streamlines

As noted before, we compute curvature directions in object space. In order to use these direction vectors as input for the streamline generation, we project them onto the image plane by applying the viewing transformation. This is done each time the algorithm reads out a direction vector, because we encountered computation errors when projecting the curvature direction in the fragment shader and storing the projected vectors in the curvature texture.

In some cases and configurations, the generation of new streamlines from a single initial one is not sufficient to fill arbitrary shapes with streamlines. It may occur that the algorithm leaves regions uncovered when starting from only one position, depending on the shape of the rendered object. This originates from the fact that the method was developed for a continuous vector field. We use multiple start candidate positions arranged in a regular grid in order to cover the whole object with streamlines.

The streamline placement algorithm of Jobard and Lefer allows to define the distance between streamlines. With creating multiple streamline sets of different streamline distances we obtain the basis for generating hatching layers of different densities. Figure 28 shows streamlines following the principal curvature directions of volume datasets.

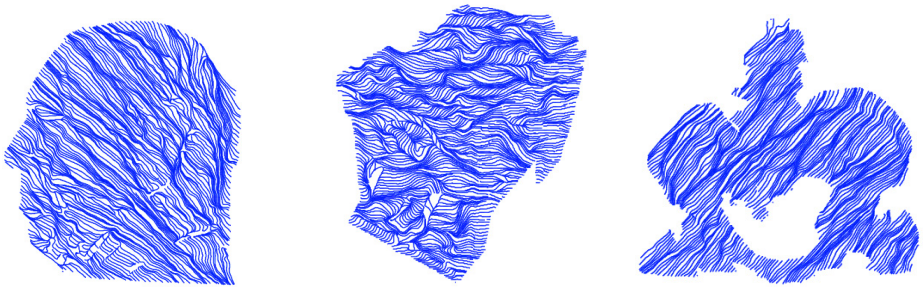

(a) (b) (c)

Figure 28: Streamlines following the principal curvature direction of (a) visible human head, (b) engine and (c) abdomen dataset.

3.5.2 Stroke Generation

We generate hatching strokes by extracting them from the streamlines simultaneously during streamline creation. As can be seen in Figure 28, streamlines entirely traverse parts of the object. Since this property is not desired for hatching strokes, one streamline is the basis for multiple strokes. At least two strokes are generated per streamline at its beginning and end. In the original streamline placement algorithm a streamline is defined by one set of points. We store multiple point arrays per streamline, each representing one stroke. We involve lighting intensity to define the length of the strokes. Lighting intensity is computed during raycasting and stored in a $2D$ texture image. Figure 29 displays such lighting intensity textures. Ambient lighting is stored in the red, diffuse lighting in the green and specular lighting contribution in the blue color channel.

To realize lighting with strokes we take account of a lighting threshold during streamline and stroke generation. Strokes are placed only in areas where brightness falls below this threshold. The threshold defines the maximum lighting intensity value where strokes are still generated. The brightness test is performed for each new point found while tracing a streamline in the vector field. The lighting intensity corresponding to a new point on the streamline is determined and compared with the threshold. If the lighting value falls below the threshold, the new point is added to the point array of the current stroke. If the lighting value exceeds the threshold, the

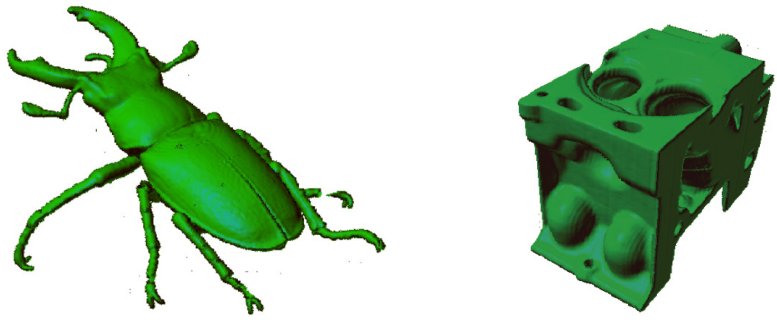

(a) (b)

Figure 29: Lighting intensity textures of (a) stagbeetle and (b) engine dataset.

current stroke point array is complete. We initialize a new stroke point array at the position where the lighting intensity falls below the lighting threshold again. The algorithm is analogous to following a streamline with a pen and drawing only in dark areas.
The lighting intensity value to be compared with the threshold is computed as the squared average of the ambient, diffuse and specular lighting components. We square the lighting intensity average to emphasize areas of low intensity (values are normalized to the range of $[0, 1]$).

3.5.3 Stroke Rendering

We use the technique presented in Section 3.2 for rendering the hatching strokes. When applying the stroke rendering method to hatching strokes, three stroke properties are taken into account. The first is a minimum number of points defining a stroke. The second is the appropriate order of the points. The third property is the lighting intensity represented by the stroke. Drawing a hatching stroke as textured spline additionally requires selecting adequate control points from the stroke's point array.
Our stroke generation method might produce strokes defined by a small number of points. To avoid drawing very short strokes or stipples, we involve a threshold during hatching stroke rendering. This value defines the minimum number of points required for a valid hatching stroke. A stroke is drawn only if its number of points exceeds this threshold.

As the generation of a streamline starts at an arbitrary point on the line and integrates the vector field in two opposite directions, the order of points in the streamline stroke's array does not necessarily match the required stroke drawing direction. We have to ensure that the streamline stroke points are processed in the proper order. Therefore we include the constraint that all hatching strokes have to be drawn from dark to bright areas. To achieve this, we read out the lighting intensities corresponding to the first and the last point of a stroke's point array. If the lighting intensity at the first point is above that of the last point, we invert the processing order of the point array for control point extraction.

In addition to determining the length of strokes according to the tone, we involve lighting during stroke rendering. We want to achieve the effect of applying more color in darker areas. We therefore pass the lighting intensity values at the beginning and end of a stroke to the stroke rendering routine. We adjust the alpha values of the brush-textured quads according to the corresponding brightness. As we draw a relatively high amount of quads we can achieve smooth tone transitions within a stroke.

We have to make a selection of control points from the stroke's point array for a spline representation. This is realized by picking points as control points in fixed intervals. The variation in the length of strokes does not raise a problem, since our stroke rendering algorithm is capable of processing splines with a different number of control points. Selecting a subset of the streamline points as control points results in smoothing curvature irregularities and discontinuities. This smoothing operation is advantageous for producing visually pleasant strokes. We also experimented with drawing strokes along the streamlines directly using the streamline points. Due to curvature irregularities and discontinuities inherent in most volume datasets this yields noisy strokes. Smoothing the streamline strokes by drawing them along Bézier curves achieves better results.

3.5.4 Hatching Layers

With the methods described in the previous sections we are able to render a hatching drawing for one level of brightness. The application of a lighting threshold during stroke generation from streamlines yields strokes in areas with a lighting intensity below the threshold. For producing pen-and-ink style illustrations rendering one level of tone is sufficient. Hatching strokes in a pen-and-ink illustration usually represent just one level of brightness. Shading with different tones and a transition between darker and brighter regions within the shading is usually not desired. Renderings in the style of pen-and-ink illustrations can be generated with our system using just one hatching layer. Since we focus on mimicking pencil hatching images, we want our volume hatching system to be capable of rendering transitions between areas of different lighting intensity. In order to achieve this we use four layers of hatching strokes. Each layer represents one level of lighting intensity or tone. In dark areas we draw short strokes of high density, brighter areas are rendered with longer strokes of lower density. Each hatching layer is computed in a separate rendering pass. The four layers are overlaid to produce the final hatching image.

We control the length of the strokes for each layer using the lighting threshold for stroke extraction from the streamlines. This allows for adjusting the length of the hatching strokes to the level of tone the layer represents. We use a low lighting threshold for the darkest level and a higher threshold value for the brightest level. These two values are linearly interpolated for the two levels in between. By modifying the lighting thresholds the brightness and contrast of the hatching drawing can be controlled. The distance between the two thresholds defines the degree of lighting variation between the four hatching layers.

To control the hatching stroke density the separating distance between the streamlines is altered. We control the brightness of each level through stroke density. Darker areas contain more hatching strokes than brighter ones. Creating streamlines with a small separating distance yields strokes of high density. The definition of a separating distance for each hatching layer is done analogous to the definition of lighting thresholds: we define a low value for the darkest level and a higher value for the brightest level. We

interpolate these two values for the levels in between. Figure 30 shows an example of four hatching layers generated with the discussed techniques.

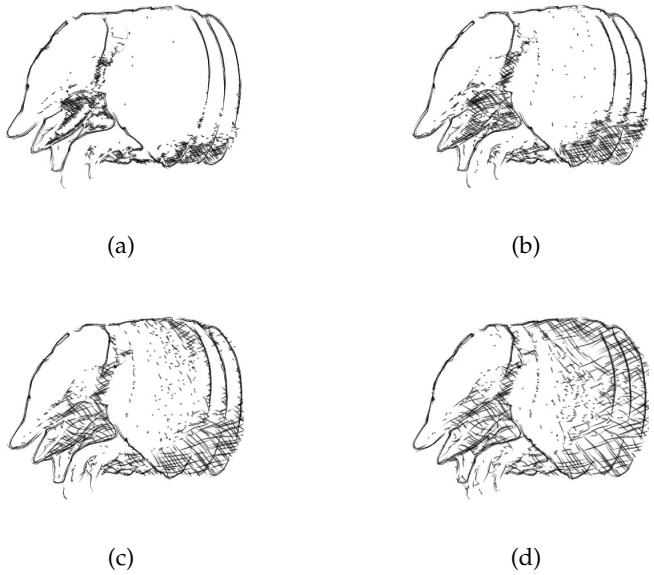

(a) (b)

(c) (d)

Figure 30: Different hatching layers for the armadillo dataset which are composed for the final hatching image. The darkest tone is represented by (a), increasing tone value to (d).

For comprehensibility the hatching layers in Figure 30 differ considerably in stroke density. For the result images in Chapter 5 we use hatching layers with a more similar density.
We originally intended to create the distinct hatching layers for trilinear texture interpolation on a fragment basis. The idea was to compute the color value of a fragment according to the corresponding brightness by interpolating between the two adequate layers. Experiments with this approach resulted in blurred hatching strokes. Drawing the layers directly yields better results because the hatching strokes maintain their original shape.

The major drawback of this approach is that it requires four passes of streamline generation. This severely affects the computational performance of our volume hatching system. A strategy for avoiding this would be to create only one set of strokes in the highest density and selecting subsets of this strokes for the brighter layers. Hereby the difficulty of selecting evenly-spaced strokes is encountered. Generating streamlines and strokes for each layer individually yields equidistant strokes inherently. We propose further optimization strategies in Chapter 7.

3.5.5 Crosshatching

Crosshatching is a drawing technique which uses strokes in different orientations to emphasize dark regions in the drawing. Crosshatching techniques differ in the directions of the crosshatching strokes. Some drawers prefer perpendicular crosshatching strokes, others draw a crosshatching with strokes slightly rotated to the original ones. It is a technique for creating expressive drawings, because it improves the perception of differently lit regions and enhances the communication of spatial relations.
We integrate crosshatching by generating further hatching layers with the methods discussed above. The only component which has to be changed for crosshatching is the curvature direction during streamline generation. We use a stroke direction for crosshatching which is perpendicular to the original stroke direction in image space. Manual crosshatching often uses a constant angle between hatching and crosshatching strokes, so we decided to adopt this technique. For obtaining a direction perpendicular to the principal curvature direction in image space, we simply rotate the projected principal curvature direction by 90 degrees. This is done during fetching the curvature direction from the curvature texture. Moreover, this mechanism allows to control the angle between original hatching strokes and crosshatching strokes. The drawing technique of slightly rotated crosshatching strokes can be realized easily.
We apply a crosshatching pass for the layers representing darker areas. In this manner we implement a technique that uses crosshatching for assisting the differentiation of regions of different brightness.

The main drawback of this crosshatching approach is that it requires an additional streamline generation as well as a stroke determination and rendering pass for each layer of crosshatching. This naturally affects performance. In addition to the four hatching passes required for the layered hatching algorithm, one to four passes are performed for crosshatching. Figure 31 displays a result image of our hatching system. Further results will be presented later on.

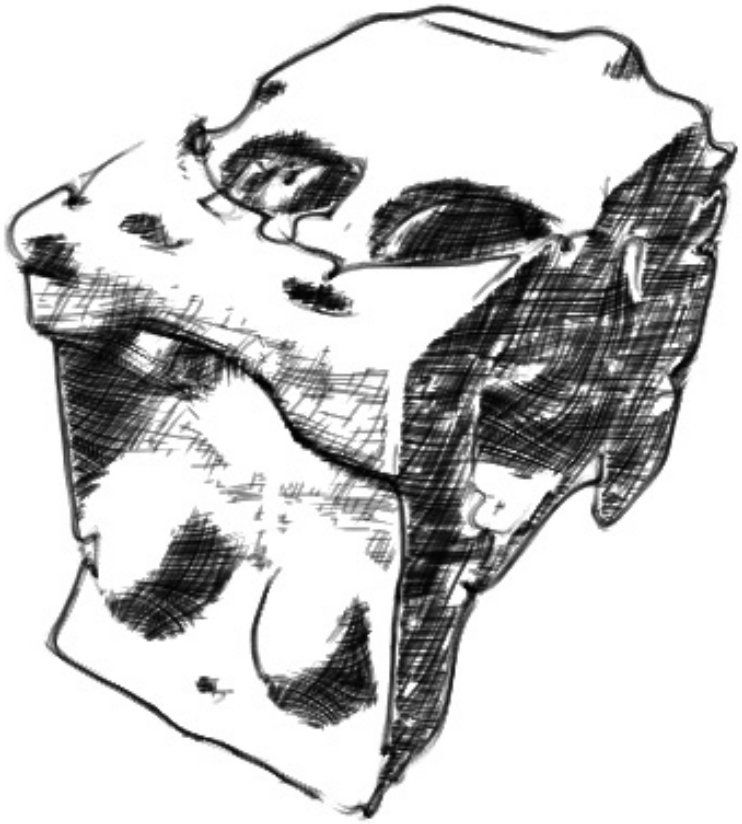

Figure 31: Crosshatching drawing of engine dataset.

3.6 Volumetric Hatching

The techniques presented in the previous sections are capable of producing hatching drawings of iso-surfaces within volume datasets. Due to using a raycasting system and traversing the volume just to one sample after the first ray-object intersection, the methods described so far are related to surfaces. The renderings used to generate hatching strokes represent the outer shell of the object specified by the transfer function. This thesis is concerned with producing volumetric hatchings and not only hatching images of the outer surface. Volumetric is used here to indicate a simultaneous visual representation of overlapping or occluded structures in the volume dataset. In this section we address the problem of volumetric hatching. We will survey two methods which serve this purpose. First we present an approach which is based on traversing the volume in segments. Then we discuss a technique which involves an analysis of the transfer function to determine relevant iso-surfaces. It generates volumetric hatchings by blending together hatching images of these iso-surfaces.

3.6.1 Segmental Raycasting

The method we initially intended to employ for volumetric hatching traverses the volume in segments. Raycasting is performed in segments or slabs. Instead of processing all samples along a ray in one step, we involve a fixed interval during raycasting. This interval defines the thickness of the segments. The segmental raycasting method requires an interleaved rendering scheme. Raycasting and hatching are performed in alternating order for each segment. The algorithm processes n samples along the ray and stores optical and spatial properties of the dataset computed from this n samples in textures. Based on these textures, hatching strokes are generated representing the visible structures within the current slab. Then the next n samples along the ray are processed and the hatching strokes for the next slab are generated. This interleaved raycasting and stroke rendering is continued until the entire volume is traversed.
The problem of this segmental approach is that it is not sensitive to the spatial arrangement of objects within the dataset. It is not well suited for displaying connected structures with hatching strokes. As the stroke gener-

ation is performed for each slab individually, objects are split in parts and these parts are hatched separately. This results in visually disconnected structures which should be drawn as a whole. Furthermore it may generate hatching strokes for unimportant parts of structures. This appears when small parts of structures are separated in an individual slab and covered with hatching strokes. If strokes are generated for the entire surface, this small parts of structures may not be perceivable due to the smoothing operations applied during curvature estimation and stroke generation.

3.6.2 Relevant Iso-Surface Detection

Due to the problems of our initial approach to volumetric hatching we developed another technique to realize the simultaneous hatched display of interior and exterior structures in volume datasets. This technique applies our hatching methods to multiple iso-surfaces. An analysis of the transfer function is performed to detect iso-surfaces relevant for the volumetric rendering. Contour and hatching strokes are generated for each of these surfaces, taking into account the transparencies specified by the transfer function. The hatched surfaces are overlaid to produce the volumetric hatching image.

The transfer function analysis is based on the fact that visible surfaces in a volume rendering are defined by maxima of the transfer function. We exploit this property to detect iso-surfaces which have to be rendered. The number of maxima in the transfer function defines the number of relevant iso-surfaces and therewith the number of hatching passes. The transfer function is analyzed by traversing the axis which represents the scalar values and detecting the maxima and minima of the opacity values. For each local maximum of the function we store the position of the directly preceding local minimum on the data value axis. Additionally, we store the opacity value corresponding to the maximum. The scalar values representing the local minima in the transfer function are then used as thresholds during raycasting. At the rendering pass of an iso-surface related to a maximum we take the preceding minimum as a threshold. This threshold affects the transfer function readout at a resample location in the raycaster. If the scalar value at a resample location falls below the threshold, we return an opacity value of zero at the transfer function readout. In this way we

skip regions of lower density as the iso-value specifying the current surface during rendering.
Transparency is realized through hatching stroke density and stroke opacity. The degree of transparency of a surface defines the amount of hatching strokes generated for this surface. Highly transparent surfaces are rendered with a small number of hatching strokes, opaque ones with hatching strokes of high density. To control the density of hatching strokes we make use of the separating distance parameter in the streamline generation routine (see Sections 3.5.1 and 3.5.3). In addition to that, we draw outer surfaces with lower opacity. Silhouette as well as hatching strokes for outer iso-surfaces are drawn less opaque in order to efficiently communicate transparencies of the different surfaces. The degree of both of these transparency visualization methods is defined by the transparency specified in the transfer function. As mentioned above, we therefore store and employ the opacity values of the transfer function maxima.
This approach functions very well for structures of high density which are occluded by structures of lower density. This characteristic is given in many organic datasets, for example bones surrounded by soft tissue. In some cases our approach is not suitable for a volumetric rendering. For instance hollow space within a structure can not be visualized properly with our approach. Therefore an enhancement of the transfer function threshold mechanism would be necessary. Rendering times increase linearly with each iso-surface determined for hatching. Our hatching routines are applied to each surface individually, therefore the computation times accumulate.
In theory, this approach is not limited to a maximum number of iso-surfaces. But for the datasets we examined, hatching more than two iso-surfaces simultaneously makes the individual iso-surfaces difficult to distinguish.
An advantage of this volumetric hatching strategy is that it offers an intuitive way of defining which objects within a dataset are to be rendered and with what opacity. The transfer function is the common tool for specifying this relations in traditional volume rendering. With adopting this concept for volume hatching, the user of our system can determine the desired volumetric properties for rendering in a familiar way.

Volumetric hatching is a technique well suited for illustration purposes due to its abstract and sparse way of conveying spatial information within volume datasets. Figure 32 presents a result image achieved with the described iso-surface detection and hatching mechanism.

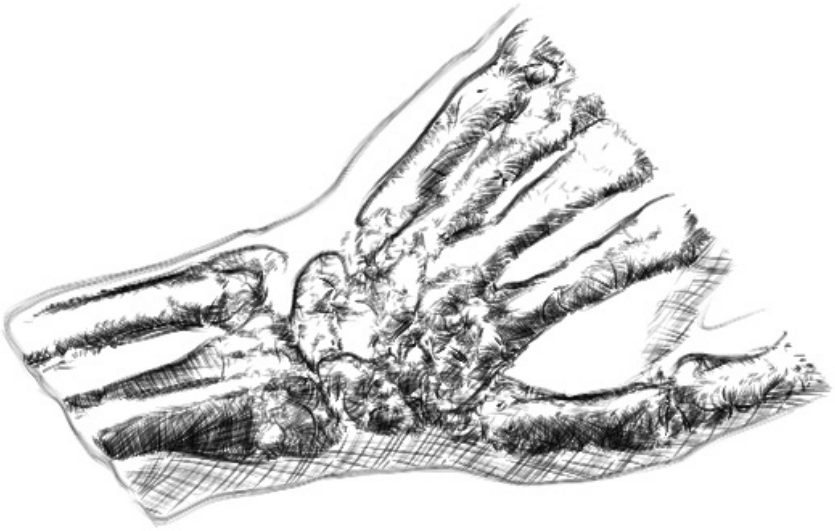

Figure 32: Volumetric hatching of hand dataset.

4 Implementation

The volume hatching system discussed in the previous chapters is implemented as a plug-in to the volume illustration software VolumeShop [2] (see Section 2.3.3). This application offers basic functionality required for the realization of the volume hatching software. A graphical user interface (GUI) as well as routines for dataset import, transfer function design and interaction are provided by VolumeShop and can be used directly. The software is written in C++ using OpenGL for graphics support, Qt as windowing toolkit and the GL Shading Language (GLSL) as shader language. In the following, we will outline the architecture of our volume hatching system by describing the basic functionality of the most important classes.

RendererVolumeHatcher

The class *RendererVolumeHatcher* is a modification of the volume rendering class of VolumeShop. It holds the objects needed for contour drawing and hatching. We will shortly present the processing order of the main rendering loop provided by this class. First the shader programs for raycasting are executed and reference information on contours, lighting and curvature are rendered to $2D$ textures using an OpenGL framebuffer object. Then these textures are filtered in fragment shaders. The following operations are executed on the CPU. We therefore copy the reference textures from graphics memory to main memory using OpenGL texture data reading functions. Subsequently silhouette drawing and hatching are performed by calling the corresponding methods of the dedicated classes.

ContourDrawer

The class *ContourDrawer* provides functionality for drawing contours with overlapping strokes (see Section 3.1). The algorithms for contour point detection (see Section 3.1.3) and contour stroke generation (see Section 3.1.4) are implemented as described in the related sections. These routines are not suited for parallel execution for graphics hardware exploitation and are therefore processed on the CPU. Contour strokes are rendered using the class *Stroker*.

Hatcher

The class *Hatcher* serves the purpose of producing hatching strokes (see Section 3.5). It controls the layered hatching scheme (see Section 3.5.4) by executing the corresponding methods of the class *Streamlines*. This involves the generation of streamlines following the principal curvature direction (see Section 3.5.1) and the simultaneous extraction of hatching strokes from the streamlines (see Section 3.5.2). Hatching strokes are subsequently rendered with the class *Stroker* calling a method which fulfills the conditions required therein (see Section 3.5.3).

Stroker

Stroke rendering methods are encapsulated and implemented in the class *Stroker*. It provides the mechanism for drawing strokes as textured splines (see Section 3.2). Contour and hatching strokes rendering routines are separated to provide the possibility of rendering contours and hatching in different styles. We employ the Developers Image Library (DevIL) [58] for importing the brush texture images. OpenGL texture mapping is utilized for displaying the textured quads.

Figure 33 shows a screenshot of VolumeShop with the plug-in for volume hatching. For adjusting the volume hatching as desired some GUI elements were integrated. This enables the user to modulate contour and hatching stroke width and opacity, hatching density and lighting interactively with sliders.

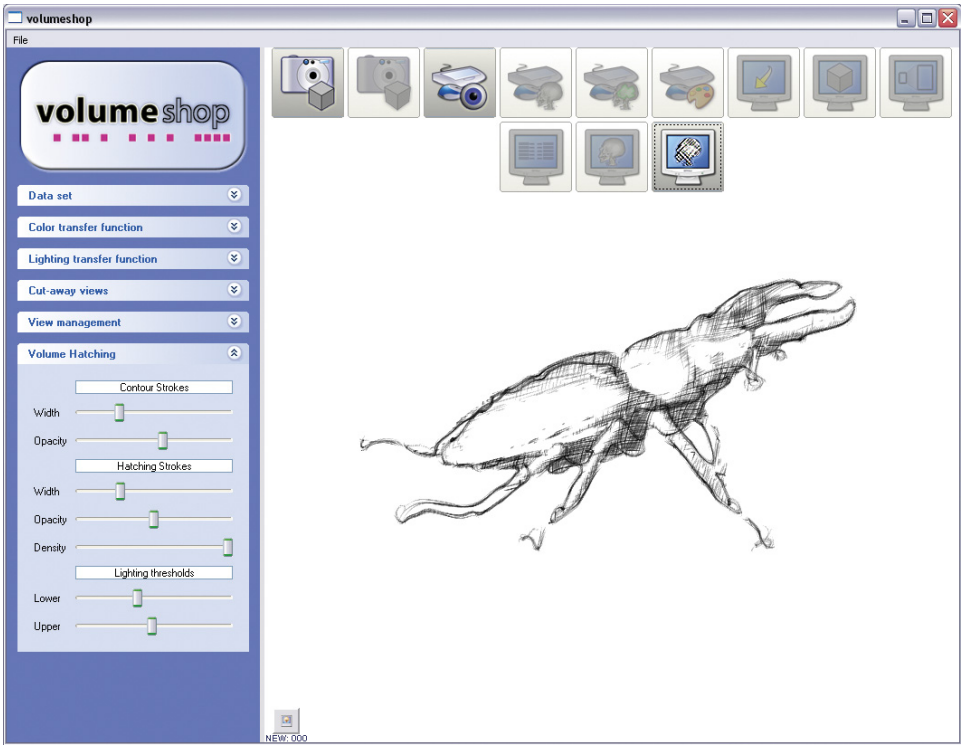

Figure 33: Screenshot of VolumeShop with volume hatching plug-in. The sliders on the left are GUI elements for altering the hatching parameters.

5 Results

In this chapter we discuss the results of our volume hatching system. Advantages and limitations of our approach will be examined. We present result images and evaluate their quality in terms of two criteria. On the one hand we address aesthetic aspects, as artistic appearance and attraction. On the other hand we examine applicability for illustration purposes. We demonstrate how the visual appearance of the images can be modified by modulating various rendering parameters. Furthermore rendering performance will be discussed.

5.1 Contour Drawing

In the following we present result images of our contour drawing approach as described in Section 3.1. We illustrate how different parameters of this technique can be employed to gain various results. Advantages and drawbacks of our spline based line-following approach will be illuminated.
For better comprehensibility we shortly recapitulate our contour drawing approach. First a contour image is rendered during raycasting. Scanlines serve to find start points on the contour. Beginning at these start points we recursively trace the contours and generate seed points in fixed intervals. We select subsets of these seed points as control points for drawing overlapping textured splines.
The selection of stroke control points involves an increment which defines the amount of skipped points in the seed point array for each new stroke. By modulating this increment a variation of the number of contour strokes can be achieved. This can be used for generating a sparser representation of the silhouette, since drawing fewer strokes results in a more sketchy appearance. Figure 34 shows contour drawings of the stagbeetle dataset with increasing increment during stroke extraction from the contour seed point array.

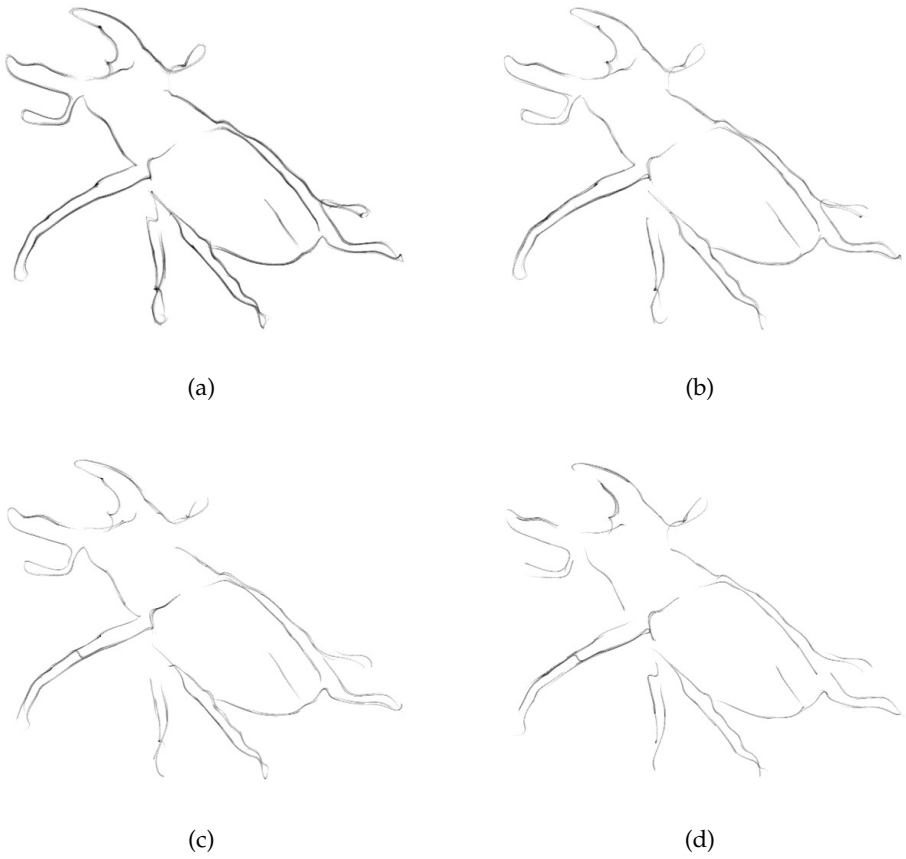

Figure 34: Variation of stroke number by modulating the increment for stroke control point selection. Increment of (a) 2, (b) 4, (c) 6 and (d) 10 points in the contour seed point array.

As noted in Section 3.1 our silhouette renderer produces errors and deviations due to inaccuracies during line following and stroke extraction. In Figure 34 these errors are recognizable as missing and incorrectly connected contour lines, for instance at the left middle leg of the stagbeetle. Although this inaccuracies might be misleading in some cases, it can also enhance the hand-drawn effect of the contour renderings in general. The hand-drawn impression can be further amplified by the method demonstrated in Figure 34 if a sparse outline is desired. The strategy of using multiple overlapping strokes instead of line primitives is capable of stylization and of mimicking hand-drawn outlines which slightly deviate from the extracted silhouette.

Another possibility for varying the number of contour strokes is to modify the interval used for seed point placement during contour following. This interval defines the number of contour locations skipped for seed point placement. A value of 1 means that a seed point is generated at each contour location found during line tracing. With a value of 2 every second position is used for placing a seed point and so on. The interval defines the distance between adjacent contour seed points. Figure 35 depicts silhouette renderings of the visible human dataset with different intervals for seed point placement. The line which crosses the face is a property of the dataset.

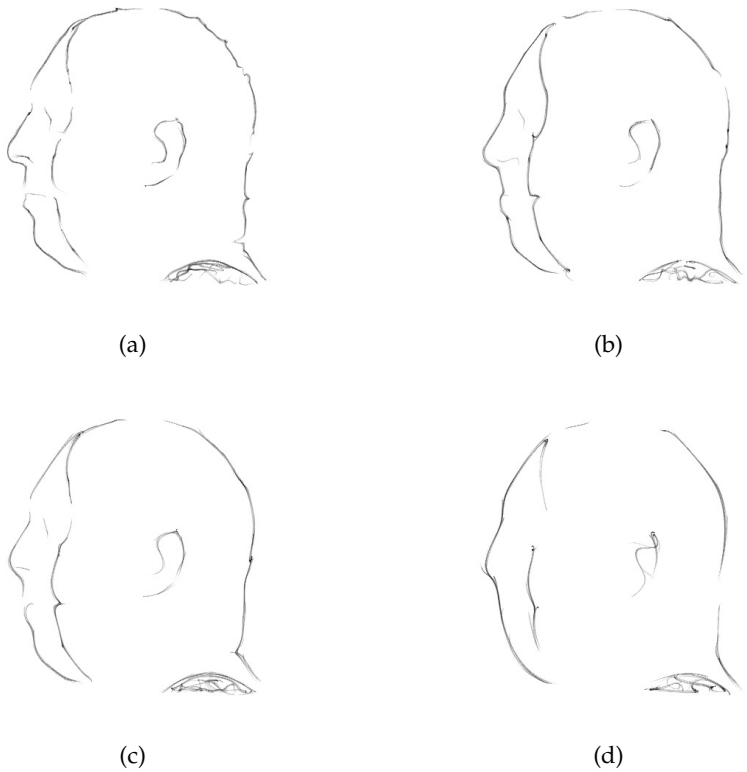

(a) (b)

(c) (d)

Figure 35: Variation of stroke number by modulating the interval for seed point placement during contour tracing. Interval of (a) 1, (b) 2, (c) 3 and (d) 5 contour positions taken during line following.

An increase of the distance between seed points for contour strokes can be used to achieve higher levels of abstraction in the contour rendering. This can be applied for instance when multiple surfaces are depicted simultaneously and the outermost surface should be rendered in an abstract form.
The contour images presented so far are all generated applying methods for adding irregularities to the strokes. We now address these methods in detail. One technique for adding randomness to a stroke is to displace the last control point of the stroke in a random direction and to propagate this displacement to the other control points. This results in a deviation of the stroke from the contour. The degree of deviation is controlled by a maximum displacement distance specified in pixels. We use an increasing degree of stroke deviation for the images in Figure 36.

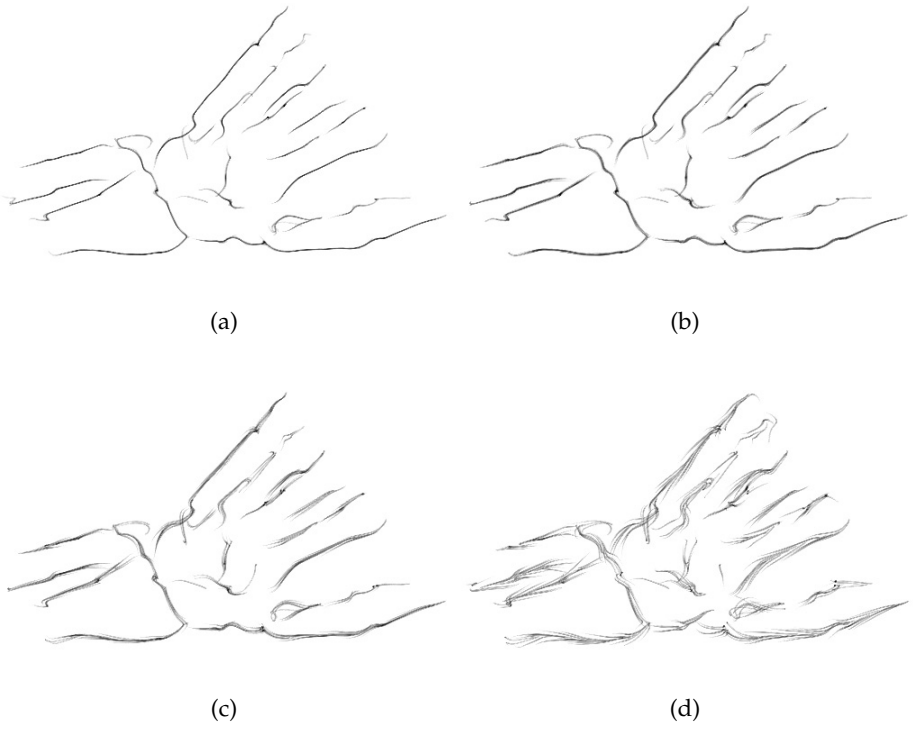

Figure 36: Variation of stroke deviation. Maximum displacement of (a) 0, (b) 2, (c) 5 and (d) 10 pixels used for deviating the strokes.

Through deviation individual strokes become perceptible. This is suited for enhancing the hand-drawn appearance of our renderings. Individually perceptible contour strokes can often be found in hand drawings, when a drawer incrementally approaches and refines the outline of an object with multiple strokes. Particularly in fast-drawn sketches individual strokes are often more visible.
Another way to increase stroke irregularity is to randomly displace the control points defining the stroke. Such a perturbation results in a scribbled appearance. Figure 37 shows contour drawings of the well-known engine block dataset with varying degrees of perturbation.

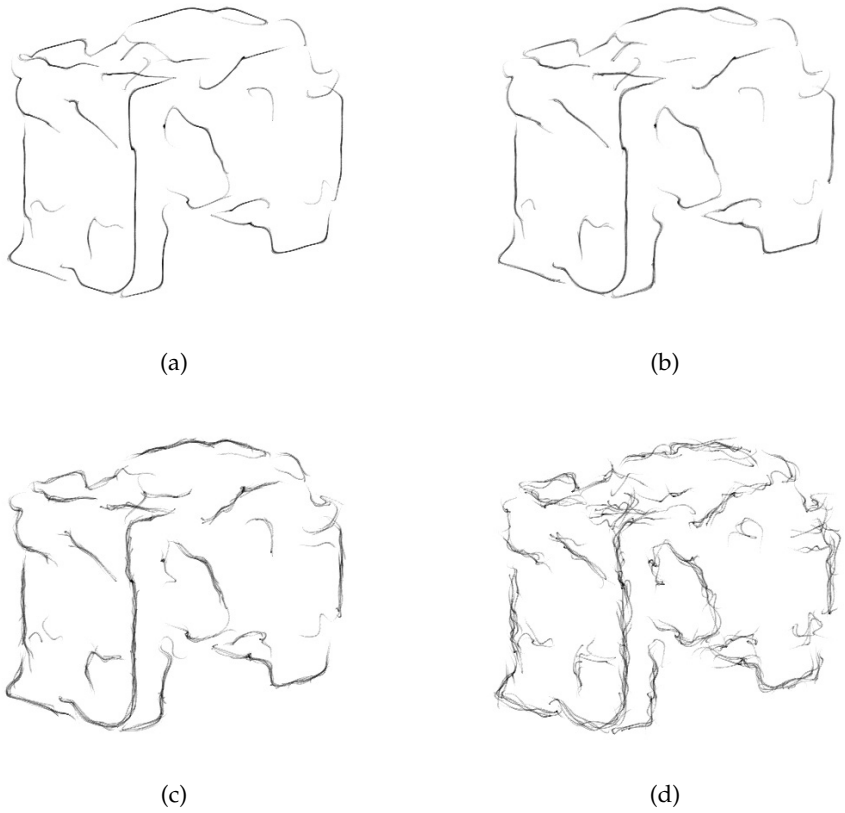

Figure 37: Variation of stroke perturbation. Maximum random displacement of (a) 0, (b) 3, (c) 7 and (d) 13 pixels of stroke control points.

The degree of control point perturbation is defined by a value which specifies the maximum displacement in pixels along the x and y axis. As we use Bézier splines for stroke rendering, their property of defining approximating curves results in rather smooth strokes even if each control point is displaced randomly.
Yet another technique to add noise to the contour rendering is to randomly translate and rotate each stroke. This also serves the purpose of disturbing the silhouette drawing and revealing single strokes for achieving a hand-drawn look. The pivot for both transformations is the first control point of a stroke. Figure 38 displays contour drawings from a tooth dataset with a rising degree of translation and rotation.

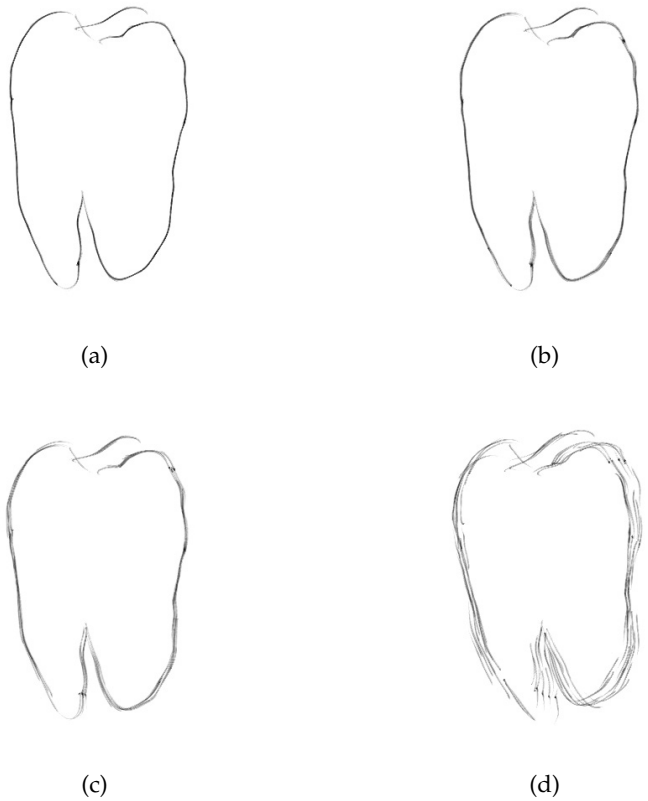

(a) (b)

(c) (d)

Figure 38: Variation of stroke translation and rotation. Maximum random translation of (a) 0, (b) 1, (c) 2 and (d) 7 pixels combined with maximum random rotation of (a) 0, (b) 2, (c) 4 and (d) 13 degrees of each stroke.

Finally, we present a contour image in larger scale to display visual properties of our contour drawing method more clearly. Figure 39 shows a contour rendering of a human head dataset.

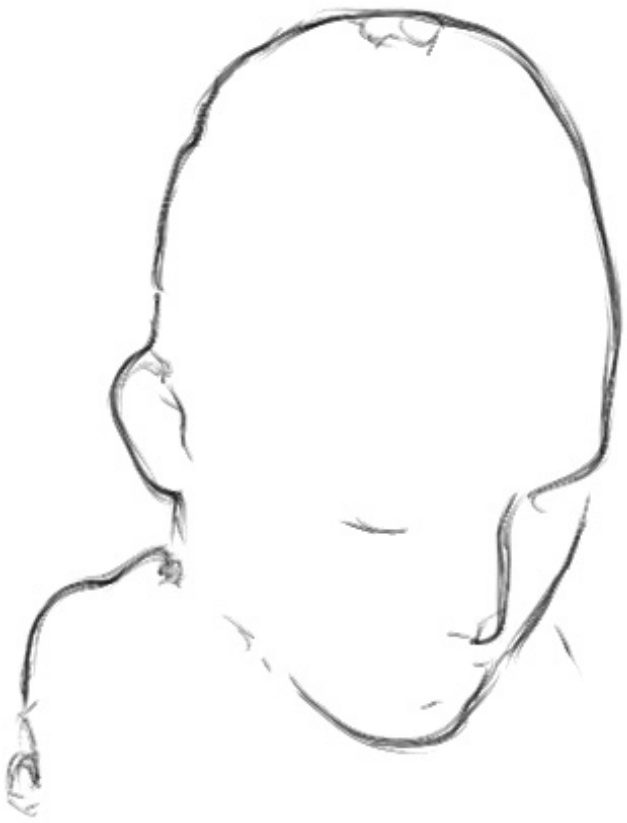

Figure 39: Contour drawing of human head dataset.

One drawback of our approach is that inner contours, such as those indicating eyes and nose in Figure 39, are detected only at certain viewpoints. Additional feature lines, such as suggestive contours [7] could remedy this problem.

For comparison, result images of other contour rendering techniques for volume data are presented. Burns et al. [3] present an approach for line drawings from volume data (see Section 2.3.4). Figure 40 displays results of this method.

(a) (b) (c)

Figure 40: Line drawings from volume data. Bonsai dataset with (a) silhouettes alone, (b) suggestive contours, (c) a different iso-surface threshold. Images courtesy of Burns et al. [3].

The approach of Nagy and Klein [37] is also concerned with silhouette rendering from volumes. It is an approach for texture-based volume rendering and allows to control the line width for enhancing the silhouettes. Result images created from the engine dataset are shown in Figure 41.

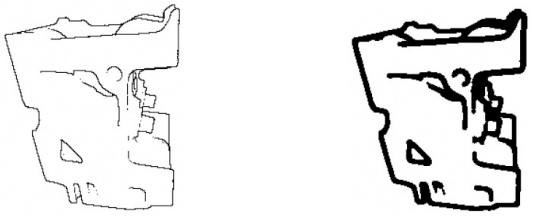

(a) (b)

Figure 41: Silhouette illustration for texture-based volume rendering. Engine dataset with (a) silhouettes and (b) enhanced silhouettes. Images courtesy of Nagy and Klein [37].

These figures illustrate the differences to our approach. While other methods give an exact visual representation of a mathematical contour definition, our method focusses on generating a more hand-drawn look. Depending on the field of application, this property may be undesired. If the application requires a precise communication of contours, the discrepancy between exact contours and our contour rendering might be intolerable. Our approach therefore provides the possibility to display the contour image gained via the dot product of gradient and viewing direction directly. The line width can be manipulated interactively, as suggested by Kindlmann et al. [23]. Furthermore we encode the inverse magnitude of the contour-defining dot product into the alpha channel to achieve a smoothing of the contour lines. Figure 42 shows an example image.

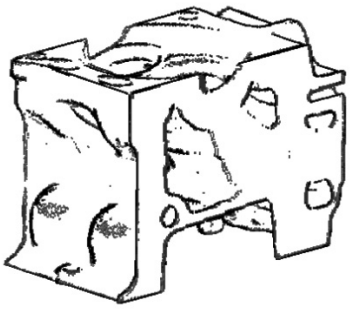

Figure 42: Silhouettes by rendering the contour image directly. Applicable if an exact representation of contours is required and deviations of stroke-based contour drawings are undesired.

On the other hand, when the application demands an artistic appearance and it is desired to simulate hand-drawn imagery, this very discrepancy is one strength of our approach. Comparing our results with traditional contour line drawings concerning hand-drawn appearance, our method results in less artificially looking images. The majority of other contour rendering methods use line primitives to depict the contours. In comparison to that, the concept of drawing multiple strokes as textured splines is better suited for achieving the impression of contours drawn by hand. Individual strokes can be rendered perceivably instead of drawing the silhouette with a continuous line. The concept of multiple strokes offers numerous possibilities for adding irregularity or randomness, as demonstrated with the

various methods. A lack of randomness is the cause for the artificial and computer-generated appearance of other line drawing methods [20].
In addition to that, other stylization for simulating different drawing media and techniques can easily be implemented. The images presented so far were all generated with a pencil-like look. In Figure 43 some possibilities for different stylization are demonstrated. They are generated by using other brush textures, stroke widths and colors.

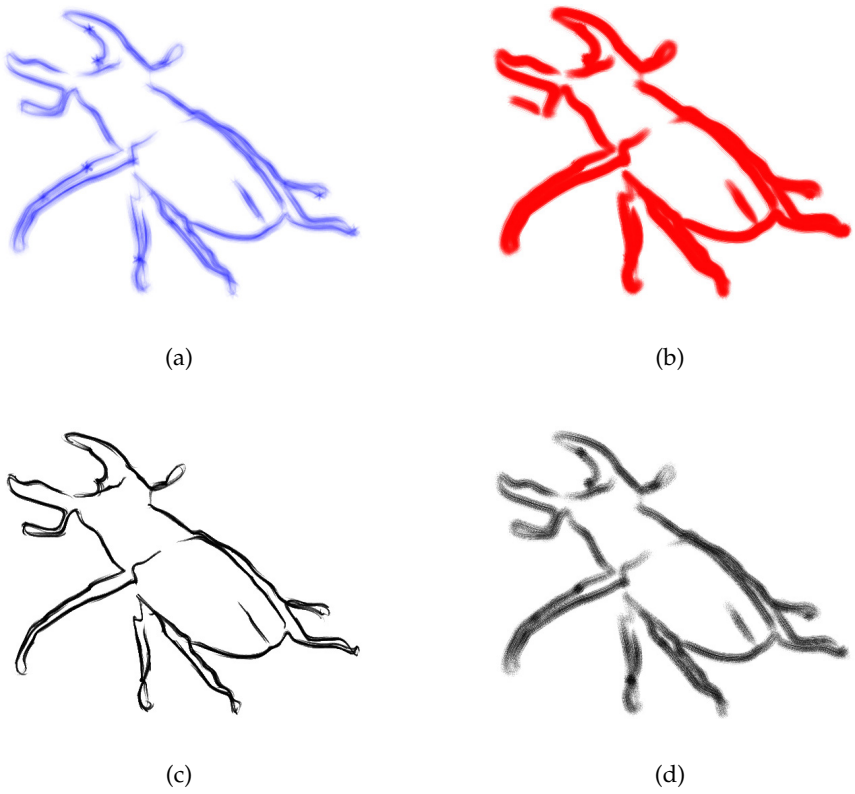

(a) (b)

(c) (d)

Figure 43: Contour drawings of the stagbeetle in different stylization by using various brush textures, stroke widths and colors.

5.2 Volume Hatching

In this section we discuss the results achieved with our volume hatching system as described in Section 3.5. We proceed with examining the outcome of our approach by showing result images and demonstrating how they can be modified with different parameters. We will point out advantages and shortcomings of our 2^+D stroke-based hatching approach.
Figure 44 depicts hatching drawings of the stagbeetle dataset with varying viewing positions.

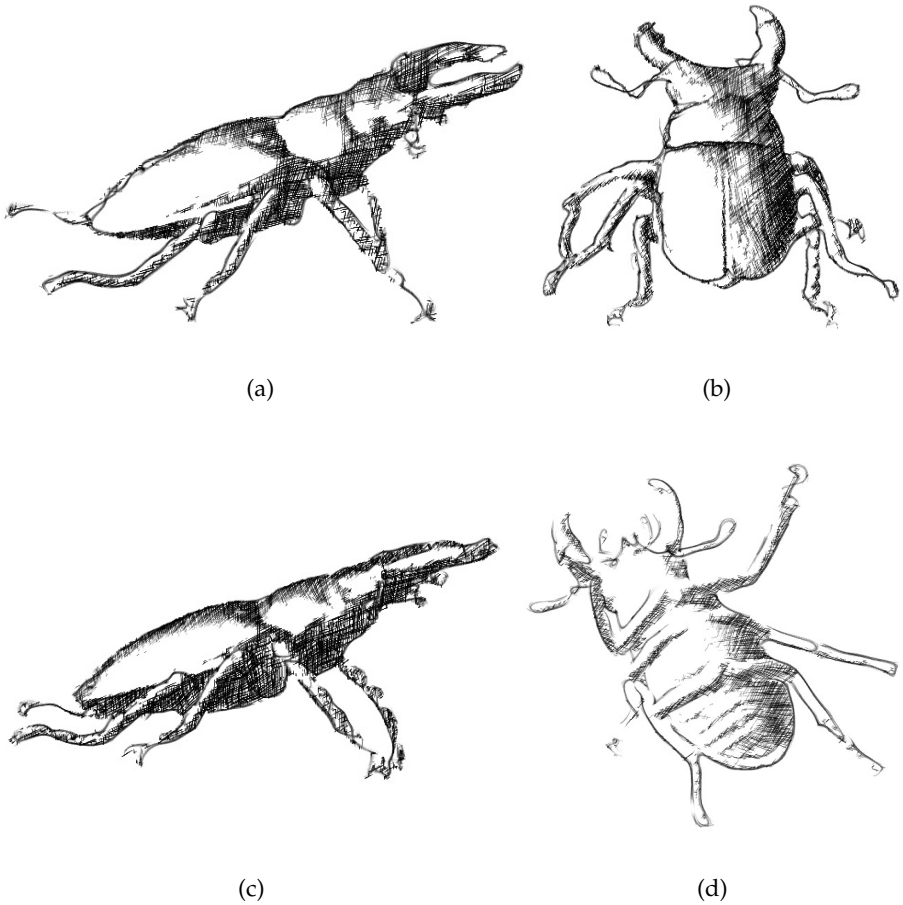

(a) (b)

(c) (d)

Figure 44: Hatching drawings of the stagbeetle dataset from different viewpoints.

Aligning hatching strokes to principal curvature directions succeeds in communicating the object's shape. It is suitable for generating strokes following the rendered surfaces. Drawing strokes as textured splines allows for mimicking the appearance of desired drawing media, in Figure 44 we chose a rendering style resembling graphite. Shading is performed with smooth transitions between areas of different tone. This is a result of rendering multiple hatching layers representing different brightness levels. Furthermore, it is noticeable in the images in Figure 44 how the strokes' opacity is modulated corresponding to the lighting intensity. The figure also features shading enhancement through the use of crosshatching layers.
Image quality is strongly dependent on the proper smoothing of the curvature direction field. We store second derivatives information in a dedicated texture which we use as direction field input for the streamline generation algorithm. Hatching strokes are extracted from these streamlines. Providing a continuous direction field is crucial for producing smooth hatching strokes. Curvature irregularities result in early termination of streamlines, since tracing the vector field stops at singularities. Besides that, it is visually disturbing if the directions of the hatching strokes differ too much. Adjacent strokes should follow a similar direction. To achieve this, we smooth the curvature texture by applying multiple Gauss filtering to eliminate high frequencies in the direction signal. Figure 45 illustrates how the number of iterations of this filtering affects the outcome.

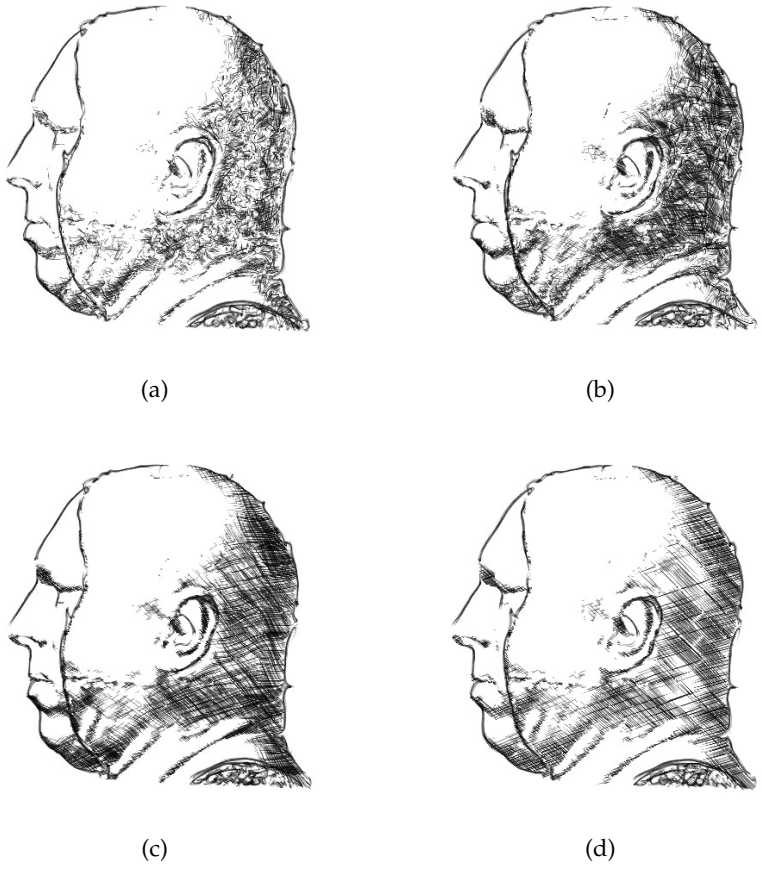

Figure 45: Hatching the visible human head with a varying number of curvature filter passes. Applying (a) 1, (b) 5, (c) 10 and (d) 20 iterations of Gauss filtering to the curvature direction field.

In Figure 45(a) curvature discontinuities result in short and noisy strokes due to lack of smoothing. With the increasing number of low-pass filtering iterations, strokes become more continuous and even (Figure 45(b)). An adequate smoothing of the curvature image is achieved in Figure 45(c). Here the strokes are oriented along the surface curvature as expected from a drawing. They are bend rather homogenously but still communicate the object's shape. Figure 45(d) demonstrates that filtering the direction field too much leads to a loss of curvature information.

Our crosshatching approach uses additional hatching layers with an adequate modification of the curvature direction during streamline generation (see Section 3.5.5). For the hatching images of the engine dataset in Figure 46 we used an increasing number of crosshatching layers.

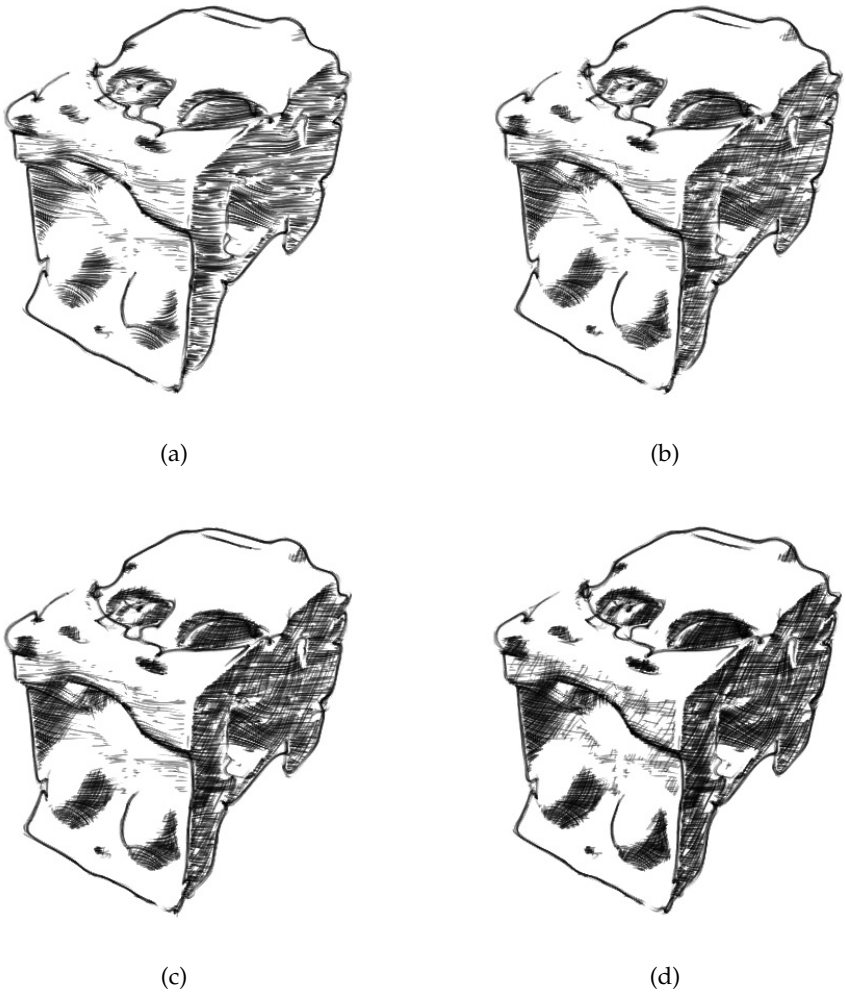

(a) (b)

(c) (d)

Figure 46: Engine dataset with different numbers of crosshatching layers. Enhancement of hatching with (a) 0, (b) 1, (c) 2 and (d) 4 crosshatching layers.

The addition of crosshatching layers results in a more pronounced shading in the engine dataset renderings. Variations of lighting intensity are emphasized by shading regions of darker tone with more hatching strokes. Applying crosshatching layers achieves a higher stroke density which is a common way of communicating dark tones within a drawing. Furthermore, crosshatching improves the hand-drawn appearance of the images, as it is a technique the observer unconsciously relates with hand drawing. Our crosshatching implementation suffers from the drawback that an additional hatching layer has to be created for each level of crosshatching, which results in an increase of rendering time.
The adjustment of brightness in the rendering by involving illumination during stroke generation is exemplified in Figure 47.

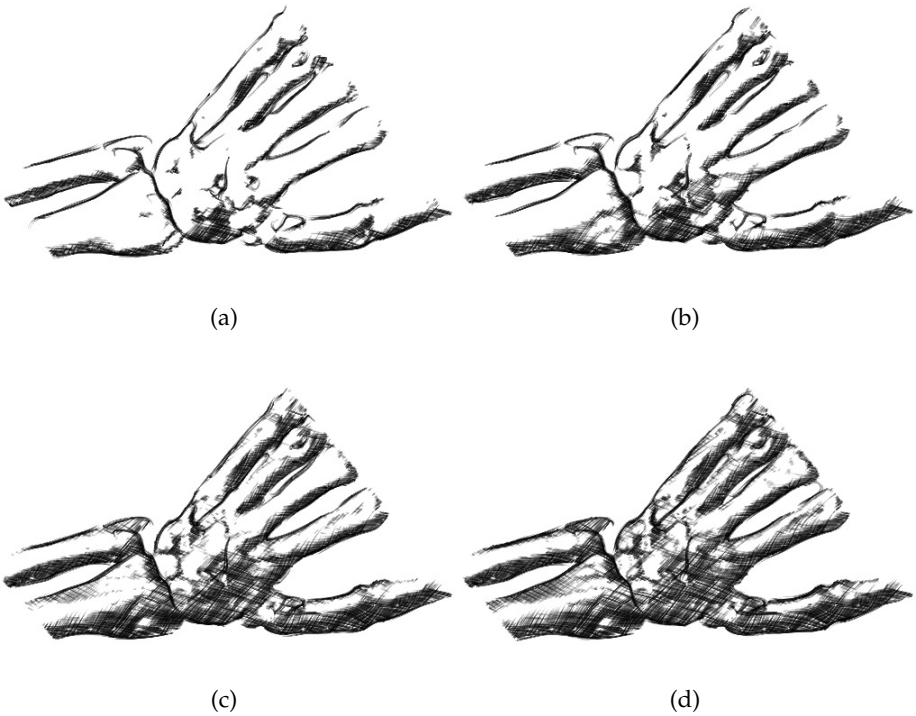

Figure 47: Variation of brightness by applying different lighting thresholds during stroke generation. Minimum/Maximum lighting thresholds of (a) 0.02/0.03, (b) 0.03/0.06, (c) 0.05/0.1 and (d) 0.07/0.12.

Figure 47 illustrates our system's capability of generating hatching drawings of different tone levels with adjustable brightness transitions. The brightness of the hatching is controlled by adapting the length of the hatching strokes corresponding to the lighting intensity. We achieve this by introducing thresholds at the stroke generation during streamline tracing (see Section 3.5.2). Since we use multiple hatching layers with increasing brightness, we define a minimum and maximum threshold. The effect of varying these lighting thresholds is illustrated in Figure 47. The relatively small threshold values (values are normalized to the range of $[0, 1]$) are due to the fact that we square lighting intensity for the threshold comparison. Besides, we take the average of ambient, diffuse and specular lighting, where our optical model produces very low ambient and specular contributions. The lighting threshold values can be interactively altered with sliders in our graphical user interface, which enable the user to tune the shading as desired.

Lighting and shading in the hatching drawings are dependent on the position of the light source. We demonstrate how a variation of the light position affects the result images in Figure 48. For the other images we employ a light position at the upper left, following a common drawing convention.

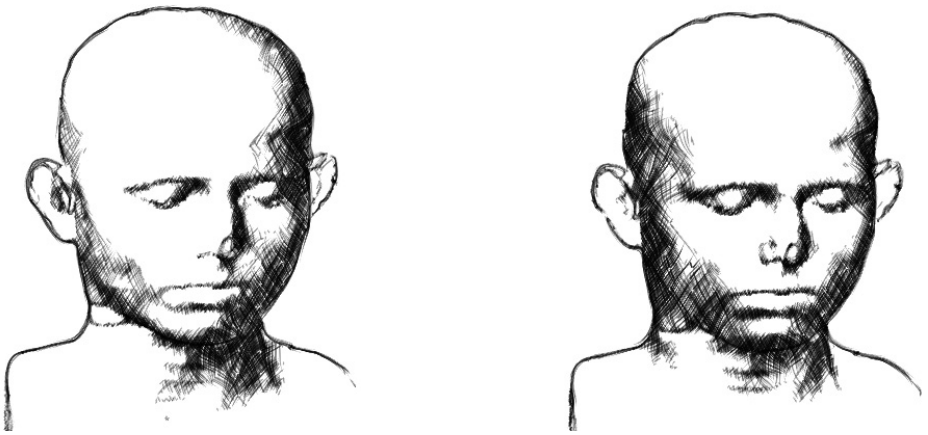

(a) (b)

Figure 48: Hatching drawings of head with varying light positions. Placement of light source at (a) upper left and (b) top.

The images presented so far were all stylized imitating pencil or graphite as drawing medium. The hatching mechanism was configured for these images to produce a hand-drawn pencil hatching with multiple brightness layers and overlapping strokes in high density. We now demonstrate that our volume hatching system is also capable of generating images in the style of pen-and-ink illustrations as commonly found in textbooks. Figure 49 shows examples of such hand-drawn pen-and-ink illustrations.

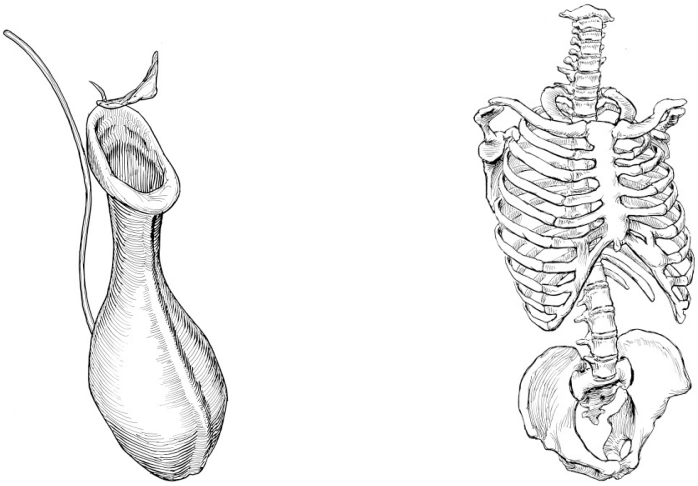

Figure 49: Examples for hand-drawn pen-and-ink illustrations. Images courtesy of Isenberg et al. [20].

To achieve a similar rendering style, we use only one hatching layer for shading the object in a sparser or more abstract way. Furthermore we avoid stylizing the strokes by texturing and attenuating them and draw them as line primitives instead. Figure 50 displays examples for this technique.

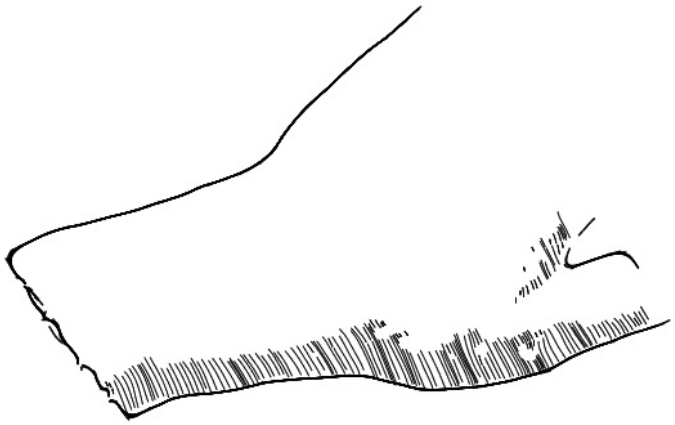

(a)

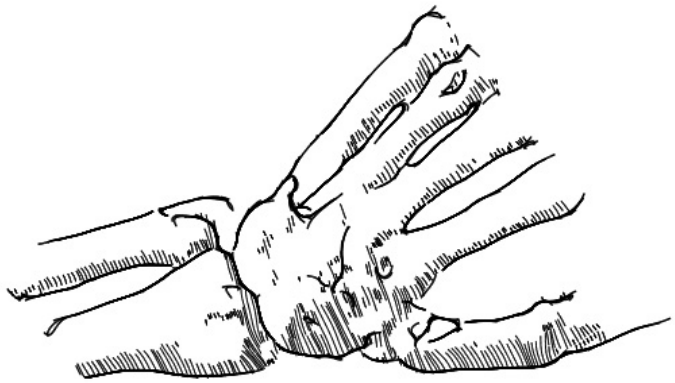

(b)

Figure 50: Pen-and-ink illustrations of hand dataset. Achieved by drawing only one layer with a sparse stroke arrangement and using line primitives instead of stylized strokes.

This pen-and-ink rendering style is well suited for demonstrating how the spacing between hatching strokes can be controlled. We specify the spacing between strokes through the separating distance during streamline generation. Figure 51 shows renderings of the tooth dataset with varying distances between strokes.

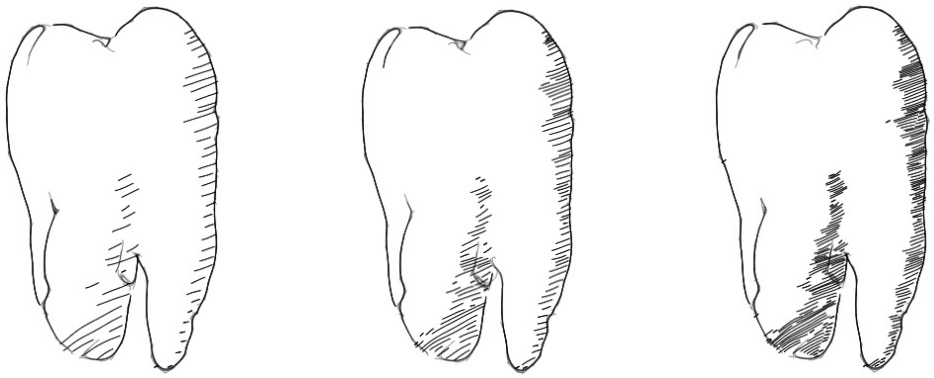

(a) (b) (c)

Figure 51: Variation of spacing between hatching strokes. Separating distance of (a) 6, (b) 3, (c) 2 pixels.

The hatching strokes in Figure 51 are not entirely evenly spaced. This is a property of the streamline generation algorithm. When streamlines are created in high density as in Figure 51(c), this variation of distance between strokes is hardly visible.

The images show that our system allows the generation of hatching images in the style of pen-and-ink illustrations as known from textbooks and other educational or illustrative areas. One possible application of our approach is the automated generation of textbook illustrations from volume datasets.

An advantage of this pen-and-ink rendering style is that it achieves high computational performance, as only one hatching layer is required. This enables interactive volume exploration at multiple frames per second on commodity hardware.

Figure 52 shows further stylization options, such as different brush textures, stroke widths, colors and stroke arrangements. Additional results are depicted in Figures 53 - 55.

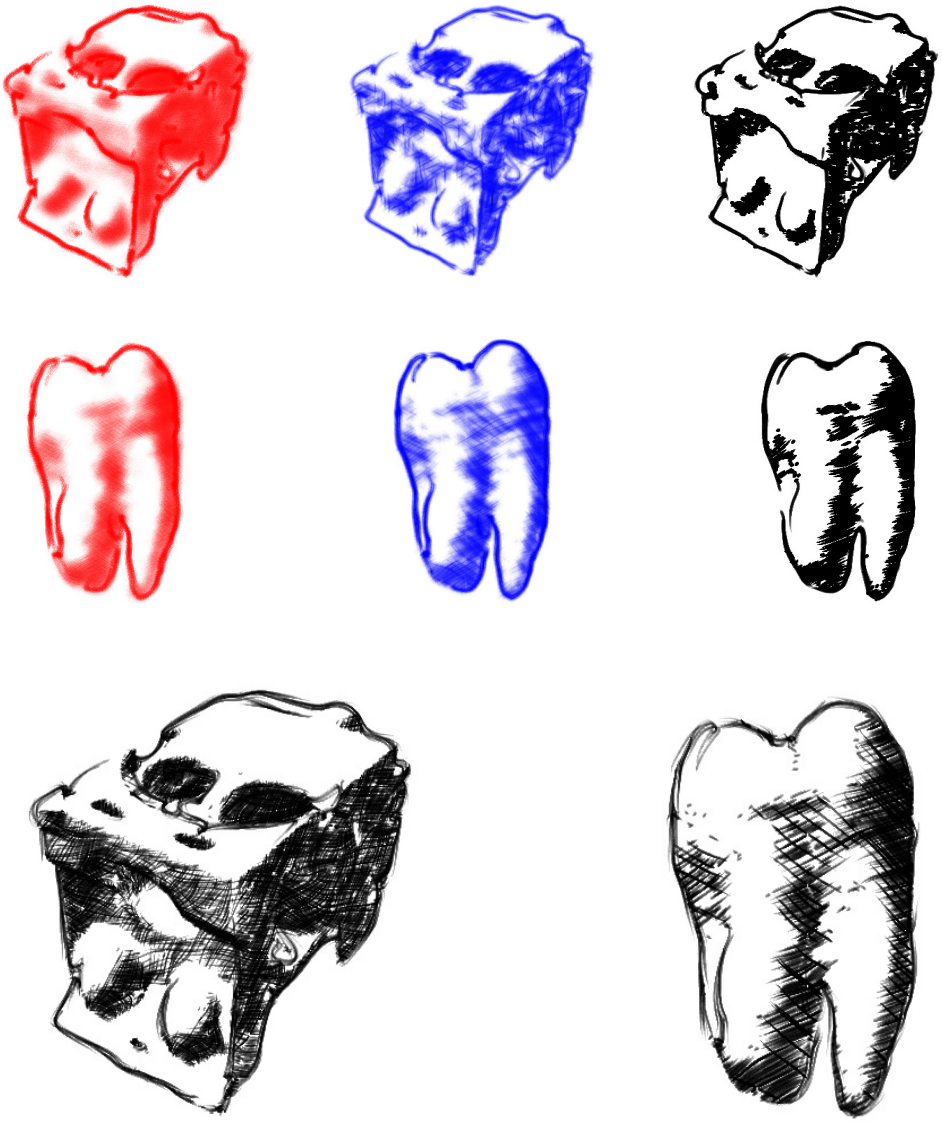

Figure 52: Different hatching stylization methods.

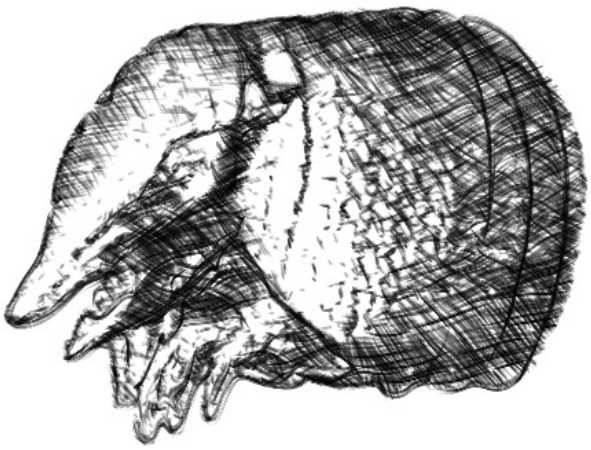

(a)

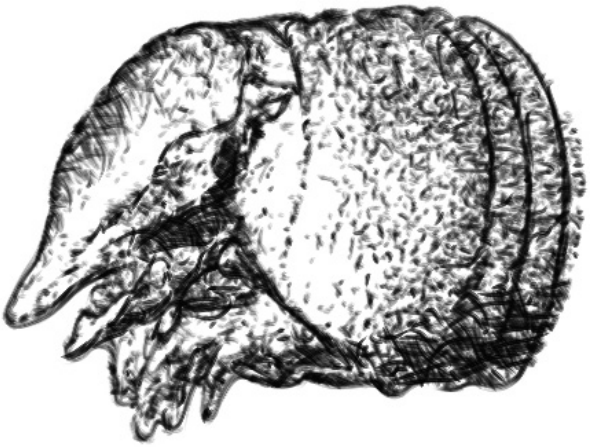

(b)

Figure 53: Hatching drawings of armadillo dataset. Image (a) has a higher degree of curvature smoothing than (b).

(a)

(b)

Figure 54: Hatching of a fly's head. Image (a) has a smaller hatching stroke width and opacity than (b).

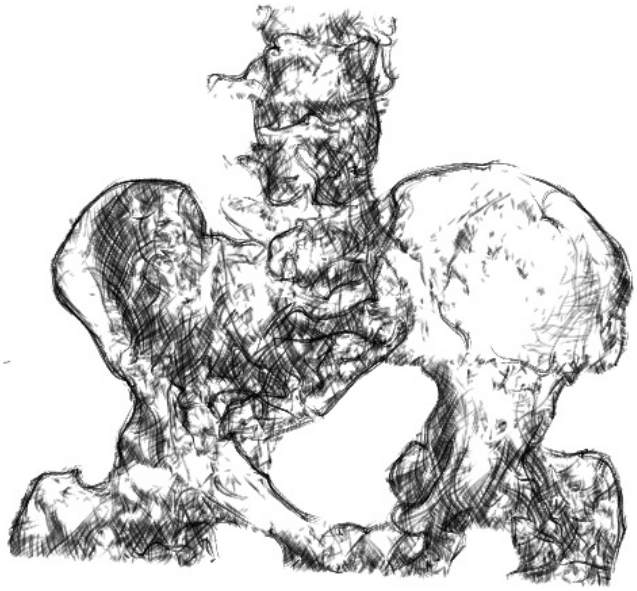

(a)

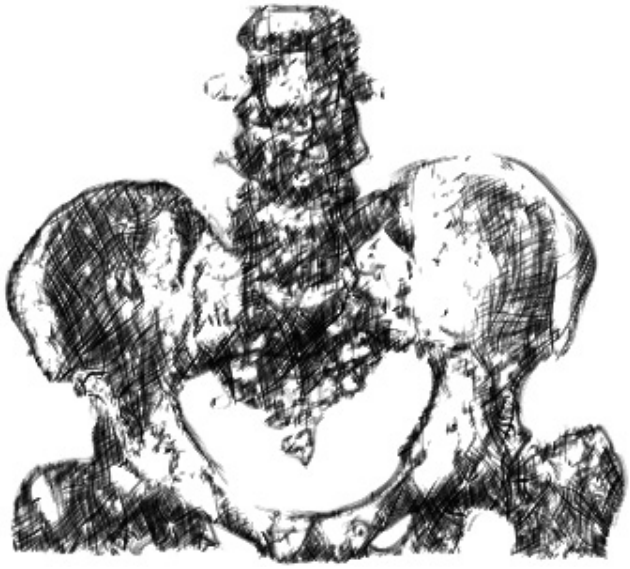

(b)

Figure 55: Hatching drawings of human pelvis. Image (a) has a smaller hatching stroke width and opacity than (b)

In the following we present result images of our volumetric hatching approach as discussed in Section 3.6. Transparency of a surface is realized by a sparser and less opaque hatching. By drawing hatching strokes for transparent objects in lower density and less opaque we enable the observer to look inside these objects. Volumetric hatching is a technique to illustrate multiple objects within a volume dataset simultaneously. Due to the abstract nature of hatching drawings they are capable of communicating important spatial information while omitting irrelevant details. The level of abstraction for outer structures can be increased by rendering just their contours without hatching. Examples for volume hatching are given in Figures 56 - 60.

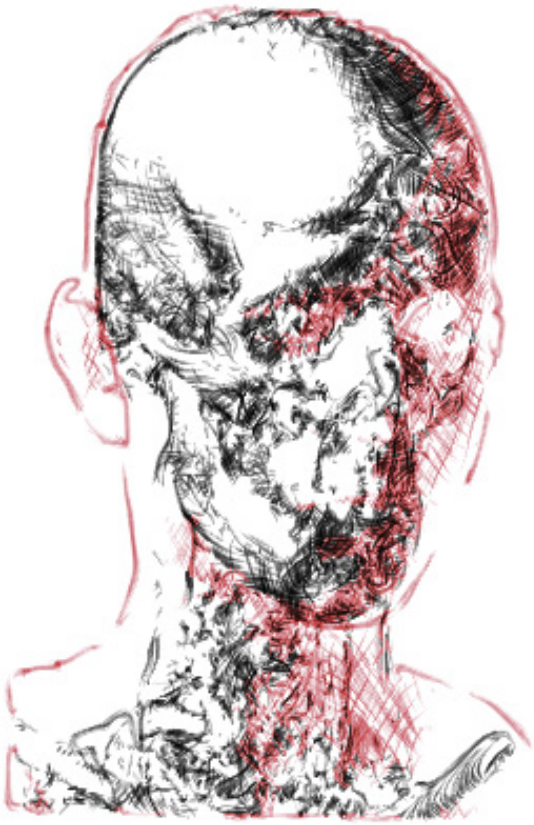

Figure 56: Volumetric hatching of human head. Using different colors for different surfaces shall ease the discrimination of objects.

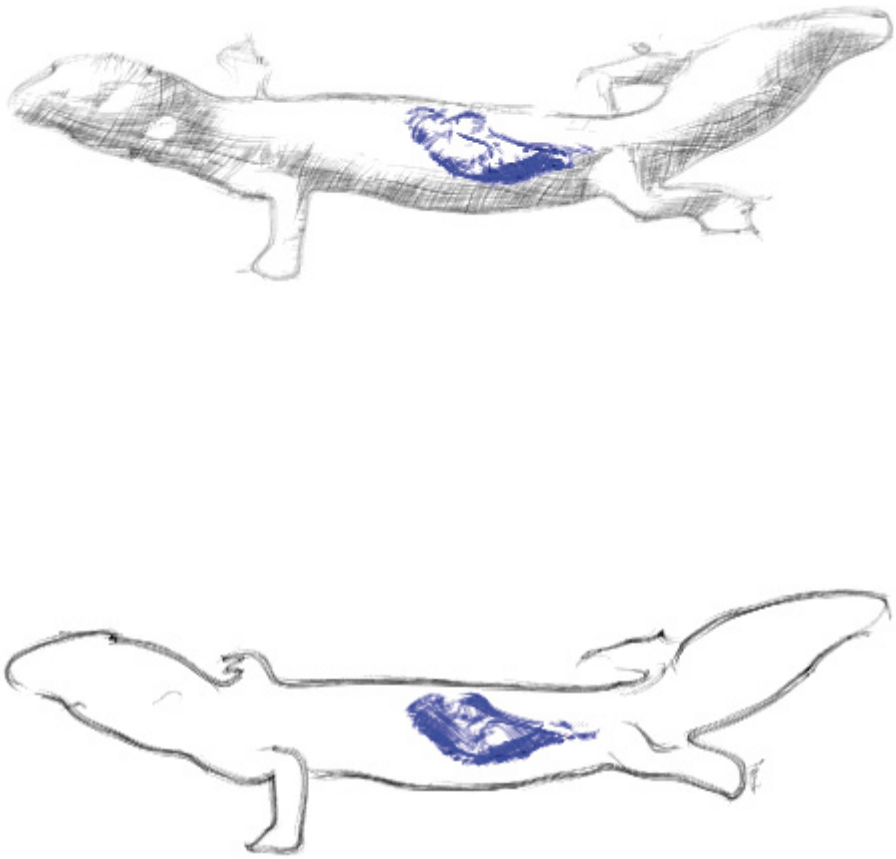

Figure 57: Volumetric hatching of leopard gecko. Interior structure is emphasized by using a different color.

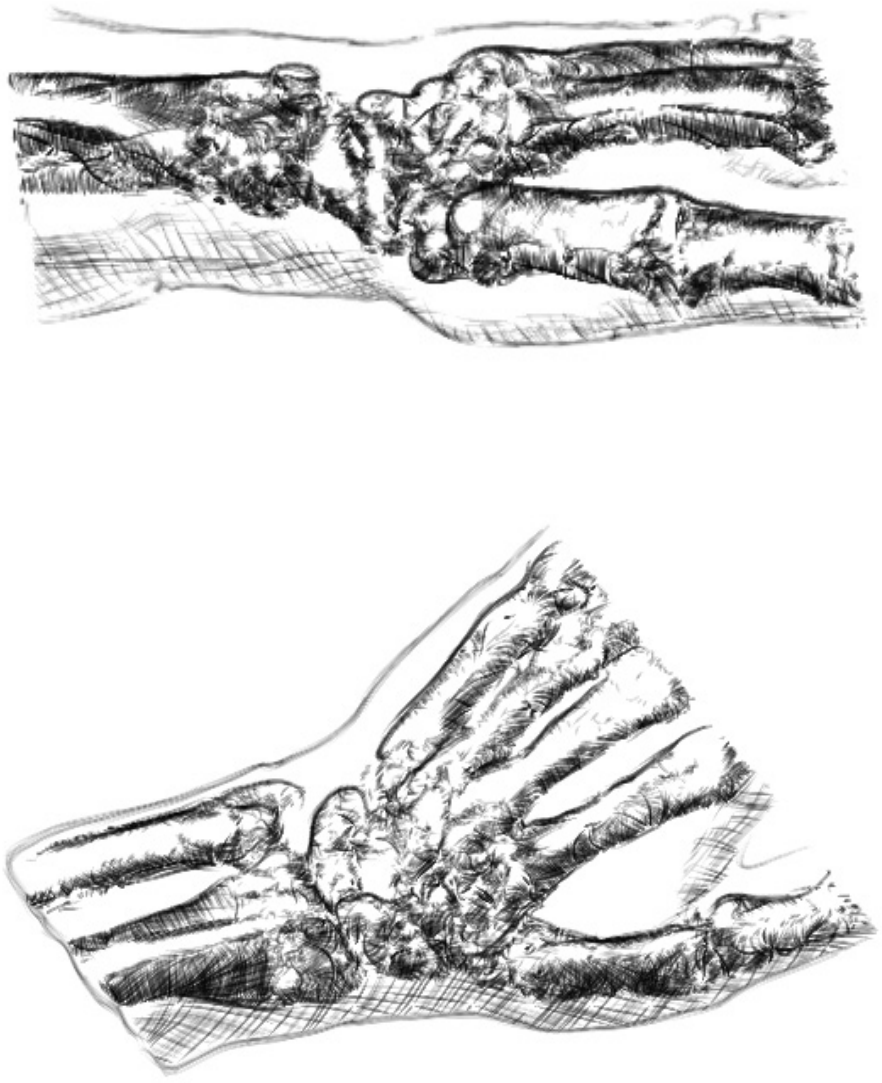

Figure 58: Volumetric hatching of human hand.

Figure 59: Volumetric hatching of human abdomen.

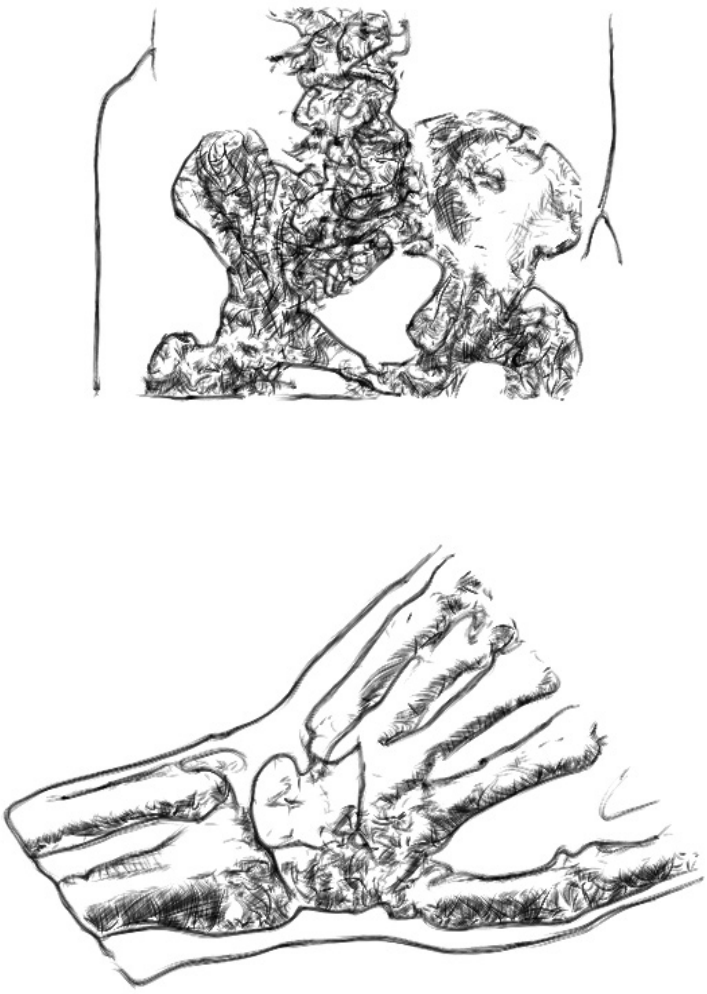

Figure 60: Volumetric hatching rendering outer surfaces only with contours and inner surfaces with hatching.

5.3 Benchmarks

This section gives an overview of the rendering times of our volume hatching application. Performance was measured on an AMD Athlon64 3800+, 1024 MB DDR Ram with a 256MB GeForce 7600 GT. Several datasets were tested. The performance discrepancy between the multi-layered hatching and the illustrative pen-and-ink hatching renderings reveals that the bottleneck of our system is the creation of multiple hatching layers. Each layer requires several texture filtering passes, a vector field integration for streamline generation and the appropriate extraction and rendering of strokes. In particular, texture filtering and streamline tracing are the most costly parts, while stroke generation and rendering have less influence. For the following benchmarks we used 5 curvature filtering passes and an integration step size of 0.9. Volumetric hatching performs worse, as hatching drawings are generated for the multiple objects separately and are then merged. Therefore the individual rendering times for the iso-surfaces add up. The rendering times given here refer to rendering only one iso-surface.
Table 1 displays time measurements taken while rendering images with the multi-layered hatching technique. This generates images as depicted in Figures 44 - 48 and in Figures 53 - 55.

dataset	dimensions	fps	sec
engine	256x256x256	0.29	3.44
tooth	256x256x161	0.76	1.32
stagbeetle	104x104x61	0.66	1.51

Table 1: Benchmarks of the multi-layered hatching technique.

Analyzing the benchmarks of rendering the hatching without crosshatching in Table 2 reveals the bottleneck of creating multiple streamline layers. As we here compute only half of the layers, one can observe a noticeable performance increase.

dataset	dimensions	fps	sec
engine	256x256x256	0.5	2.0
tooth	256x256x161	1.45	0.69
stagbeetle	104x104x61	0.98	1.02

Table 2: Benchmarks of the multi-layered hatching technique without crosshatching.

The fastest rendering speed is obtained with the pen-and-ink rendering style (see Figures 50 and 51), since we only compute one streamline layer of lower density. Table 3 shows framerates achieved with this technique.

dataset	dimensions	fps	sec
engine	256x256x256	3.28	0.3
tooth	256x256x161	5.66	0.18
stagbeetle	104x104x61	3.86	0.26

Table 3: Benchmarks of the pen-and-ink illustration technique.

These numbers demonstrate that the bottleneck of our approach is the creation of multiple hatching layers. In Section 7 we will outline strategies to remedy these problems.

6 Summary

In this chapter we summarize the most important ideas presented in this thesis.

6.1 Introduction

Non-photorealistic rendering techniques provide abstraction and stylization possibilities useful for illustrative visualization. Applying pen-and-ink techniques such as contour drawing and hatching to volume rendering can communicate spatial properties of volume data in a visually pleasant way. Images, for instance, could be more readily accepted by observers which are unfamiliar with looking inside the human body. Realistic rendering models might be perceived with distaste in this context. Another application possibility is given by the automated creation of textbook illustrations from volumetric data.

6.2 Contour Drawing

We present an image space approach for stylized contour depiction. It is based on rendering the contour with multiple overlapping strokes. Strokes are displayed with a brush texture drawn along a spline, which enables smooth strokes and various stylization possibilities. Our contour drawing technique consists of four steps. Initially, silhouette extraction is performed. Afterwards the contours are filtered. Then we use a line-following algorithm to sequentially find points on the contour. Finally, subsets of these points are selected and used as spline control points for drawing contour strokes.

For silhouette extraction we use the angle between gradient and viewing direction. We realize the concept of thickness-controlled contours suggested by Kindlmann et al. [23]. The contour detection is implemented for graphics hardware execution. An output contour image is rendered to a $2D$ texture. This contour texture is preprocessed with Gauss filtering in order to improve the result of our line-following method.

In order to detect points on the contour in a partially sequential order, we employ a recursive line-following algorithm. Initial points are detected

with scanlines. For each location we search the local pixel neighborhood for the two pixels with the highest contour value. We recursively continue at the two locations detected until no new contour position can be determined. When the recursion stops contour points are seeded in fixed intervals during backtracking, yielding equidistant points on the contour.
Afterwards stroke control points are selected from this set of partially-sequential contour points. We use splines with a variable number of control points. Starting from one point, we keep adding the successive points to a stroke until either the distance or contour direction of the next point differs too much from the last point. Control point selection for the next stroke starts at a small offset in the contour point array, so the overlapping of strokes is realized.
We use various geometrical randomization methods like stroke deviation and perturbation to achieve a hand-drawn visual appearance. Our approach does not create completely accurate and precise contours. It produces squiggles and slight deviations from the exact silhouette. This is a result of errors in the line-following and control point selection mechanisms. We argue that this randomness enhances the hand-drawn appearance of the silhouette rendering. But it can also be disturbing and misleading for some applications.

6.3 Stroke Rendering

Strokes are rendered as textured splines. We draw a stroke with multiple overlapping quads bearing a brush texture along a Bézier curve. This allows for a stylized stroke rendering capable of simulating various artistic drawing media. Width and opacity are modulated for realizing tapering and fading of strokes. Opacity of hatching strokes is defined according to the lighting intensity. Various randomization techniques allows for individualizing strokes. Drawing each stroke individually produces larger irregularities as hatching approaches which use textures containing multiple strokes. This leads to a less artificial and computer generated visual impression.

6.4 Curvature Estimation

We compute curvature information to align hatching strokes to the surface of the rendered object. We implement the algorithm proposed by Kindlmann et al. [23]. For solving linear equation systems to compute eigenvectors which represent principal curvature directions we use the Gauss-Seidel method. We smooth the curvature data with multiple Gauss filtering passes. We use a convolution kernel weighted with the curvature magnitude to implement a curvature-sensitive filtering. Curvature directions have to be smoothed properly, in order to obtain continuous and even hatching strokes and to avoid hatching too many details. All these curvature estimation and filtering operations are performed on the GPU.

6.5 Streamline-Based Volume Hatching

For realizing volume hatching we chose a stroke-based 2^+D approach. Intermediate information representing spatial and optical properties, namely curvature and lighting, is rendered to $2D$ textures. Based on this information we place and orient hatching strokes in image space. Searching for a method for generating equidistant, curvature-aligned strokes in image space, we applied Jobard and Lefer's technique [22] for creating evenly-spaced streamlines. It is a flow visualization method and creates equidistant lines following the directions specified by a $2D$ vector field. We adapted Jobard and Lefer's algorithm for our problem and generate streamlines on a curvature direction field. We simultaneously extract strokes from these streamlines and render them as textured splines. We use multiple streamline sets to create hatching layers representing regions of different lighting intensities.
For generating volumetric representations, we apply this hatching technique to multiple iso-surfaces.

6.5.1 Creating Evenly-Spaced Streamlines

We compute curvature directions in object space and afterwards project them onto the image plane. This direction field is taken as input for the evenly-spaced streamline generation algorithm of Jobard and Lefer [22].
In some cases and configurations, the generation of new streamlines from

a single initial one is not sufficient to fill arbitrary shapes with streamlines. Therefore we use multiple initial candidate positions arranged in a regular grid in order to cover the whole object with streamlines.
The streamline algorithm allows to define the distance between streamlines. With creating multiple streamline sets with different separating distances we obtain the basis for generating hatching layers of different densities.

6.5.2 Stroke Generation

We generate hatching strokes by extracting them from the streamlines simultaneously with streamline creation. One streamline is the basis for multiple strokes. We involve lighting intensity to define the length of the strokes. To realize lighting with strokes we take account of a lighting threshold during streamline generation. Strokes are placed only in areas where brightness falls below this threshold. At each new point, the corresponding lighting intensity is compared with the threshold. If it falls below the threshold, the new point is added to the current stroke. If it exceeds the threshold, the current stroke is completed. We initialize a new stroke at the position where the lighting intensity falls below the lighting threshold again.

6.5.3 Stroke Rendering

When applying the textured splines stroke rendering method to hatching strokes, three stroke properties are taken into account. The first is a minimum number of points defining a stroke. The second is the appropriate order of the points. The third property is the lighting intensity. Drawing a stroke as spline additionally requires selecting adequate control points from the stroke's point array.
Our stroke generation method might produce strokes represented by just a few points. To avoid drawing very short strokes we use a threshold defining the minimum number of points.
As the generation of a streamline starts at an arbitrary point on the line and integrates the vector field in two opposite directions, the order of points in a stroke's array does not necessarily match the required stroke drawing

direction. We have to ensure that the points are processed in the proper order. Therefore we include the constraint that all hatching strokes have to be drawn from dark to bright areas. To achieve this, we invert the processing order of the point array for control point extraction if the first point of a stroke corresponds to a higher lighting intensity than its last point.
In addition to determining the length of strokes according to the tone, we involve lighting during stroke rendering. So the effect of applying more color in darker areas is achieved. We adjust the opacity of the textured quads to the corresponding brightness.
We have to make a selection of control points from a stroke's point array for a spline representation. This is realized by selecting points as control points in fixed intervals. Selecting a subset of the streamline points as control points and drawing interpolating splines results in low-pass filtering of curvature discontinuities and generates smooth strokes.

6.5.4 Hatching Layers

With the methods described previously we are able to render a hatching drawing for one level of brightness. For producing pen-and-ink style illustrations one level of tone is sufficient, because here it is common to shade the pictured object in an abstract manner. For mimicking pencil hatching images, we achieve transitions between areas of different lighting intensity by using four layers of hatching strokes. Each layer represents one level of tone. In dark areas we draw short strokes of high density, brighter areas are rendered with longer strokes of lower density.
We control the length of the strokes for each layer by using the lighting threshold for stroke extraction from streamlines. This allows for adjusting the length of the hatching strokes to the level of tone the layer represents. We use a minimum and a maximum threshold and interpolate the values for the layers in between. With these thresholds the brightness and contrast of the hatching drawing can be controlled. The distance between the two thresholds defines the degree of lighting variation between the four hatching layers.
To control the hatching stroke density the separating distance between the streamlines is employed. Additionally to opacity modulation and stroke length we control the brightness of each level by stroke density.

6.5.5 Crosshatching

We integrate crosshatching by generating further hatching layers. The only component which has to be changed for crosshatching is the curvature direction during streamline generation. For crosshatching, we use a stroke direction which is perpendicular to the original stroke direction in image space. Manual crosshatching often uses a constant angle between hatching and crosshatching strokes, so we decided to adopt this technique. To obtain a direction perpendicular to the principal curvature direction in image space, we rotate the projected principal curvature direction by 90 degrees.

6.5.6 Volumetric Hatching

To realize volumetric hatching, in terms of a simultaneous hatched display of interior and exterior structures, we apply our hatching methods to multiple iso-surfaces. An analysis of the transfer function is performed to detect iso-surfaces relevant for the volumetric rendering. Contour and hatching strokes are generated for each of these surfaces, taking into account the transparencies specified by the transfer function. The hatched surfaces are overlaid to produce the volumetric hatching image.
The transfer function analysis is based on detecting relevant iso-surfaces through local maxima and minima of the transfer function. The number of local maxima defines the number of visible iso-surfaces and therewith the number of hatching passes. Minima are used as thresholds affecting the transfer function readout during raycasting. If the scalar value at a resample location falls below the threshold, a zero color contribution is assumed. Transparency is realized by means of hatching stroke density and stroke opacity. The degree of a surface's transparency defines the opacity and density of hatching strokes generated for this surface. The degree of transparency modulation is specified with the transfer function.
Variations of volumetric hatching include applying different rendering styles to the different surfaces or depicting outer surfaces with contours only and hatching the inner structures.

6.6 Results

We discussed the results of the volume hatching system and described its advantages and limitations. We presented result images and examined their quality in terms of aesthetics and applicability to illustration purposes. We demonstrated how the visual appearance of the images can be altered by modulating various rendering parameters. Furthermore we benchmarked rendering performance.

The majority of examples presented implement the style of hand-drawn pencil hatchings, but we also demonstrated the capability of generating abstract pen-and-ink illustrations as found in textbooks.

We showed that the major shortcomings of our approach are the inaccuracies of our contour drawing mechanism and the non-interactive framerates of multi-layered hatching. Rendering benchmarks revealed the bottleneck of creating multiple streamline layers and evidenced that interactivity is achieved if only one layer is created.

7 Conclusions and Future Work

We presented an approach capable of visualizing volumetric data with non-photorealistic rendering techniques mimicking hand-drawn hatching imagery in different artistic styles such as pencil or pen-and-ink drawing. We use this visualization method for creating volumetric hatching drawings. Our system allows for generating hatching images from volume data in various rendering stylization covering a wide spectrum from artistic hand-drawn graphite hatchings to abstract pen-and-ink illustrations as found in textbooks. One advantage of our approach is the hand-drawn appearance of our results. We try to avoid the artificial look of many computer-generated drawings, although at the cost of accuracy. We focused on achieving such an appearance and tried to design algorithms which mimic hand drawing processes. The techniques developed for this thesis provide the functionality required in possible application areas such as surgery illustration or automated creation of textbook illustrations. We discussed the result images with experts from the field of drawing. This revealed several shortcomings of our approach, but the image quality was regarded as promising.

One limitation of our system is the lack of accuracy of our contour drawing method. However, this randomness can also be beneficial as it creates a hand-drawn impression. The other drawback is that we do not achieve an interactive rendering performance. In the following, we address possibilities for further enhancing and improving our mechanisms.

The randomness of our contour rendering approach originates from the fact that our recursive line-following and stroke extraction algorithms are suboptimal. Involving a rather large neighborhood in the line searching results in false connections between adjacent contour lines. We need this large neighborhood to compensate gaps in the contour image. Gauss filtering the image too intensively to close all this gaps leads to a broadening of contours, which is also disadvantageous for the line-following algorithm. Therefore a more sophisticated contour filtering scheme would allow for decreasing the search neighborhood and would avoid the problem of falsely connected adjacent contour lines. Detecting multiple line-tracing start points with scanlines leads to a noncontinuous sequentiality within

the contour point array. The tracing algorithm starts from numerous positions and stores detected points in the same array. This makes the task of determining which contour points are selected to form strokes more difficult. One way of solving this is separately storing contour points detected at tracing the contour from one position. This would require multiple contour point arrays, one for each start point. This method would guarantee that points are provided in sequential order. In addition to that, there could be developed other ways of detecting appropriate start points to decrease their number.

With these methods, it should be possible to fix the defects of our contour renderer. But perhaps it would destroy the hand-drawn impression it achieves as a result of its faultiness. Mimicking human manufacture demands implicating human shortcomings.

We showed that the bottleneck of our approach is the creation of up to eight layers of streamlines. We originally intended to use a higher variation of stroke density for the different hatching layers and therefore created multiple streamline layers. We found out that the images look better when all layers are created in high density. Therefore the streamline layers are quite similar to each other. So generating only two layers of streamlines, one for basic hatching and one for crosshatching, could be sufficient to create images in similar quality. The concept of multiple hatching layers representing different tone levels could still be implemented, but all the strokes would have to be generated from these two sets of streamlines. By rendering the hatching layers with a slight offset for displacing them would result in a similar visual impression as creating strokes from multiple streamline layers of similar density. Rendering benchmarks given in Section 5.3 prove that our approach achieves interactive framerates if only one layer of streamlines is generated.

As the vector field integration is the most costly part of our application, another acceleration strategy is to downsample the curvature field and to trace the streamlines on a smaller image. Rendering time directly correlates with the size of the curvature vector field. Even faster and having the same effect would be to perform the volume rendering for calculating all intermediate spatial and optical information on a smaller viewport. This would achieve a high performance increase. Downsampling the curvature

field additionally implies smoothing the curvature information. Rendering time spent on multiple filtering passes could be saved. So this approach would efficiently accelerate the three most expensive computations of our implementation, namely volume rendering, curvature smoothing and vector field integration, at the same time.

Another acceleration possibility will be given in the near future by geometry shader functionality included in Shader Model 4.0. As it will be possible to create vertices on the GPU, the vector field integration and stroke generation could be executed in graphics hardware.

Realizing these optimization strategies would make it possible to perform volume hatching at multiple frames per second in a quality similar to the result images presented.

The visual similarity to artistic drawing media could be increased by applying dedicated NPR methods, for instance involving paper effects for pencil rendering as used by Lee et al. [27] (see Section 2.2.3).

In order to further improve the image quality in aesthetic aspects it will be necessary to perform extensive user studies. Furthermore, exchange with experts in drawing has to be continued. Since these people professionally deal with creating drawings, they can easily discover aesthetic shortcomings in computer-generated drawings.

Further ideas include the integration of focus+context approaches such as importance driven volume rendering in our hatching technique. These methods for emphasizing volumetric relations combined with the abstraction and stylization capabilities of volume hatching could create powerful ways of illustrating volumetric data.

Acknowledgements

First of all, I thank my supervisor Stefan Bruckner for all his support and help. I further thank Eduard Gröller and Stefan Müller for their supervision and valuable discussions. Many thanks to Otto Mittmannsgruber and Daniel v. Chamier-Glisczinski for their advice related to drawing. Finally, I want to express my gratitude to my parents for making this work possible.

References

[1] S. Bruckner, S. Grimm, A. Kanitsar, and M. E. Gröller. Illustrative context-preserving volume rendering. In *Proceedings of EuroVis 2005*, pages 69–76, 2005.

[2] S. Bruckner and M. E. Gröller. VolumeShop: An interactive system for direct volume illustration. In *Proceedings of IEEE Visualization 2005*, pages 671–678, 2005.

[3] M. Burns, J. Klawe, S. Rusinkiewicz, A. Finkelstein, and D. DeCarlo. Line drawings from volume data. *ACM Transactions on Graphics*, 24(3):512–518, 2005.

[4] B. Cabral, N. Cam, and J. Foran. Accelerated volume rendering and tomographic reconstruction using texture mapping hardware. In *Proceedings of VolVis 1994*, pages 91–98, 1994.

[5] M. S. T. Carpendale, D. J. Cowperthwaite, and F. D. Fracchia. Distortion viewing techniques for 3-dimensional data. In *Proceedings of the IEEE InfoVis 1996*, pages 46–53, 1996.

[6] C. J. Curtis, S. E. Anderson, J. E. Seims, K. W. Fleischer, and D. H. Salesin. Computer-generated watercolor. *Computer Graphics*, 31(Annual Conference Series):421–430, 1997.

[7] D. DeCarlo, A. Finkelstein, S. Rusinkiewicz, and A. Santella. Suggestive contours for conveying shape. *ACM Transactions on Graphics*, 22(3):848–855, 2003.

[8] J. Diepstraten, D. Weiskopf, and T. Ertl. Transparency in interactive technical illustrations. *Computer Graphics Forum*, 21(3):317–325, 2002.

[9] F. Dong, G. J. Clapworthy, and M. Krokos. Volume rendering of fine details within medical data. In *Proceedings of IEEE Visualization 2001*, pages 387–394, 2001.

[10] F. Dong, G. J. Clapworthy, H. Lin, and M. Krokos. Nonphotorealistic rendering of medical volume data. *IEEE Computer Graphics and Applications*, 23(4):44–52, 2003.

[11] D. S. Ebert and P. Rheingans. Volume illustration: non-photorealistic rendering of volume models. In *Proceedings of IEEE Visualization 2000*, pages 195–202, 2000.

[12] A. Van Gelder and K. Kim. Direct volume rendering with shading via three-dimensional textures. In *Proceedings of VolVis 1996*, pages 23–30, 1996.

[13] A. Gooch, B. Gooch, P. Shirley, and E. Cohen. A non-photorealistic lighting model for automatic technical illustration. In *Proceedings of SIGGRAPH 1998*, pages 447–452, 1998.

[14] B. Gooch, P.-P. J. Sloan, A. Gooch, P. Shirley, and R. F. Riesenfeld. Interactive technical illustration. In *Symposium on Interactive 3D Graphics*, pages 31–38, 1999.

[15] M. Hadwiger, C. Sigg, H. Scharsach, K. Bühler, and M. Gross. Real-time ray-casting and advanced shading of discrete isosurfaces. *Computer Graphics Forum*, 24(3):303–312, 2005.

[16] P. Haeberli. Paint by numbers: abstract image representations. In *Proceedings of SIGGRAPH 1990*, pages 207–214, 1990.

[17] H. Hauser, L. Mroz, G.-I. Bischi, and M. E. Gröller. Two-level volume rendering - fusing MIP and DVR. In *Proceedings of IEEE Visualization 2000*, pages 211–218, 2000.

[18] A. Hertzmann and D. Zorin. Illustrating smooth surfaces. In *Proceedings of SIGGRAPH 2000*, pages 517–526, 2000.

[19] V. Interrante, H. Fuchs, and S. M. Pizer. Enhancing transparent skin surfaces with ridge and valley lines. In *Proceedings of IEEE Visualization 1995*, pages 52–59, 1995.

[20] T. Isenberg, P. Neumann, S. Carpendale, M. C. Sousa, and J. A. Jorge. Non-photorealistic rendering in context: An observational study. In *Proceedings of NPAR 2006*, pages 115–126, 2006.

[21] S. Islam, S. Dipankar, D. Silver, and M. Chen. Spatial and temporal splitting of scalar fields in volume graphics. In *Proceedings of IEEE VolVis 2004*, pages 87– 94, 2004.

[22] B. Jobard and W. Lefer. Creating evenly-spaced streamlines of arbitrary density. In *Proceedings of Eurographics Workshop on Visualization in Scientific Computing '97*, pages 43–56, 1997.

[23] G. Kindlmann, R. Whitaker, T. Tasdizen, and T. Möller. Curvature-based transfer functions for direct volume rendering: Methods and applications. In *Proceedings of IEEE Visualization 2003*, pages 513–520, 2003.

[24] G. Knittel. The UltraVis system. In *Proceedings of VolVis 2000*, pages 71–79, 2000.

[25] A. Krüger, C. Tietjen, J. Hintze, B. Preim, I. Hertel, and G. Strau. Interactive visualization for neck-dissection planning. In *Proceedings of EuroVis 2005*, pages 295– 302, 2005.

[26] P. Lacroute and M. Levoy. *Fast Volume Rendering Using a Shear-Warp Factorization of the Viewing Transformation*. PhD thesis, Stanford University, Computer Systems Laboratory, 1995.

[27] H. Lee, S. Kwon, and S. Lee. Real-time pencil rendering. In *Proceedings of NPAR 2006*, pages 37–45, 2006.

[28] M. Levoy. Display of surfaces from volume data. *IEEE Computer Graphics and Applications*, 8(3):29–37, 1988.

[29] M. Levoy. Efficient ray tracing of volume data. *ACM Transactions on Graphics*, 9(3):245–261, 1990.

[30] M. Levoy. Volume rendering by adaptive refinement. *The Visual Computer*, 6(1):2–7, 1990.

[31] E. B. Lum and K.-L. Ma. Hardware-accelerated parallel non-photorealistic volume rendering. In *Proceedings of NPAR 2002*, pages 67–74, 2002.

[32] L. Markosian, M. A. Kowalski, S. J. Trychin, L. D. Bourdev, D. Goldstein, and J. F. Hughes. Real-time nonphotorealistic rendering. In *Proceedings of SIGGRAPH 1997*, pages 415–420, 1997.

[33] M. McGuire and J. F. Hughes. Hardware-determined feature edges. In *Proceedings of NPAR 2004*, pages 35–147, 2004.

[34] M. Meißner, U. Hoffmann, and W. Straßer. Enabling classification and shading for 3D texture mapping based volume rendering using OpenGL and extensions. In *Proceedings of IEEE Visualization 1999*, pages 207–214, 1999.

[35] K. Mueller and R. Crawfis. Eliminating popping artifacts in sheet buffer-based splatting. In *Proceedings of IEEE Visualization 1998*, pages 239–246, 1998.

[36] K. Mueller, N. Shareef, J. Huang, and R. Crawfis. High-quality splatting on rectilinear grids with efficient culling of occluded voxels. *IEEE Transactions on Visualization and Computer Graphics*, 5(2):116–134, 1999.

[37] Z. Nagy and R. Klein. High-quality silhouette illustration for texture-based volume rendering. In *Proceedings of WSCG 2004*, pages 301–308, 2004.

[38] Z. Nagy, J. Schneider, and R. Westermann. Interactive volume illustration. In *Proceedings of VMV 2002*, pages 497–504, 2002.

[39] S. Parker, M. Parker, Y. Livnat, P.-P. Sloan, C. Hansen, and P. Shirley. Interactive ray tracing for volume visualization. *IEEE Transactions on Visualization and Computer Graphics*, 5(3):238–250, 1999.

[40] E. Praun, A. Finkelstein, and H. Hoppe. Lapped textures. In *Proceedings of SIGGRAPH 2000*, pages 465–470, 2000.

[41] E. Praun, H. Hoppe, M. Webb, and A. Finkelstein. Real-time hatching. In *Proceedings of SIGGRAPH 2001*, pages 581–586, 2001.

[42] C. Rezk-Salama, K. Engel, M. Bauer, G. Greiner, and T. Ertl. Interactive volume rendering on standard PC graphics hardware using multi-textures and multi-stage rasterization. In *Proceedings of the Workshop on Graphics Hardware 2000*, pages 109–118, 2000.

[43] Z. Salah, D. Bartz, and W. Straßer. Illustrative rendering of segmented anatomical data. In *Proceedings of SimVis 2005*, pages 175–184, 2005.

[44] M. P. Salisbury, S. E. Anderson, R. Barzel, and D. H. Salesin. Interactive pen-and-ink illustration. In *Proceedings of SIGGRAPH 1994*, pages 101–108, 1994.

[45] J. Schumann, T. Strothotte, S. Laser, and A. Raab. Assessing the effect of non-photorealistic rendered images in CAD. In *Proceedings of SIGCHI 1996*, pages 35–41, 1996.

[46] S. Stegmaier, M. Strengert, T. Klein, and T. Ertl. A simple and flexible volume rendering framework for graphics-hardware-based raycasting. In *Proceedings of the International Workshop on Volume Graphics 2005*, pages 187–195, 2005.

[47] M. Straka, M. Cervenansky, A. La Cruz, A. Köchl, M. Sramek, M. E. Gröller, and D. Fleischmann. The VesselGlyph: Focus & context visualization in CT-angiography. In *Proceedings of IEEE Visualization 2004*, pages 385–392, 2004.

[48] J. Sweeney and K. Mueller. Shear-warp deluxe: the shear-warp algorithm revisited. In *Proceedings of the Joint EUROGRAPHICS - IEEE TCVG Symposium on Visualization 2002*, pages 95–104, 2002.

[49] J.-P. Thirion and A. Gourdon. Computing the differential characteristics of isointensity surfaces. *Computer Vision and Image Understanding*, 61(2):190–202, 1995.

[50] J.-P. Thirion and A. Gourdon. The 3d marching lines algorithm. *Graphical Models and Image Processing*, 58(6):503–509, 1996.

[51] S. M. F. Treavett and M. Chen. Pen-and-ink rendering in volume visualisation. In *Proceedings of IEEE Visualization 2000*, pages 203–210, 2000.

[52] I. Viola and M. E. Gröller. Smart visibility in visualization. In *Proceedings of EG Workshop on Computational Aesthetics in Graphics, Visualization and Imaging*, pages 209–216, 2005.

[53] I. Viola, A. Kanitsar, and M. E. Gröller. Importance-driven volume rendering. In *Proceedings of IEEE Visualization 2004*, pages 139–145, 2004.

[54] M. Webb, E. Praun, A. Finkelstein, and H. Hoppe. Fine tone control in hardware hatching. In *Proceedings of NPAR 2002*, pages 53–58, 2002.

[55] R. Westermann and T. Ertl. Efficiently using graphics hardware in volume rendering applications. In *Proceedings of SIGGRAPH 1998*, pages 169–178, 1998.

[56] L. Westover. Footprint evaluation for volume rendering. *Computer Graphics*, 24(4):367–376, 1990.

[57] G. Winkenbach and D. H. Salesin. Computer-generated pen-and-ink illustration. *Computer Graphics*, 28(Annual Conference Series):91–100, 1994.

[58] D. Woods. DevIL: A full featured cross-platform image library. http://openil.sourceforge.net/, 2006.

List of Figures

List of Tables